NACA RM L52A29

RESEARCH MEMORANDUM

WIND-TUNNEL INVESTIGATION OF THE AERODYNAMIC CHARACTERISTICS IN PITCH OF WING-FUSELAGE COMBINATIONS AT HIGH SUBSONIC SPEEDS

ASPECT-RATIO SERIES

By Richard E. Kuhn and James W. Wiggins

Langley Aeronautical Laboratory
Langley Field, Va.

NATIONAL ADVISORY COMMITTEE
FOR AERONAUTICS

WASHINGTON
April 1, 1952

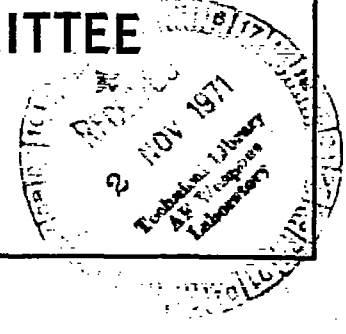

NATIONAL ADVISORY COMMITTEE FOR AERONAUTICS

RESEARCH MEMORANDUM

WIND-TUNNEL INVESTIGATION OF THE AERODYNAMIC CHARACTERISTICS IN PITCH OF WING-FUSELAGE COMBINATIONS AT HIGH SUBSONIC SPEEDS

ASPECT-RATIO SERIES

By Richard E. Kuhn and James W. Wiggins

SUMMARY

An investigation was conducted in the Langley high-speed 7- by 10-foot tunnel to determine the effect of aspect ratio on the aerodynamic characteristics in pitch of wing-fuselage combinations with 45° sweepback at the quarter-chord line and 0.6 taper ratio at high subsonic speeds. Generally good agreement was obtained between the theoretical wing-fuselage and wing-alone lift-curve slopes and the experimental data, although the absolute magnitudes given by the wing-alone theory were somewhat low. The experimental wing-fuselage aerodynamic-center variation with aspect ratio agreed fairly well with wing-fuselage theory at a low Mach number for which the comparison was made. The results showed little variation of the aerodynamic center with Mach number up to the force-break Mach number. Above this point all wings exhibited a rapid rearward movement of the aerodynamic center. The drag-rise Mach number tended to increase slightly with increase in aspect ratio. Below drag rise, the zero-lift drag (wing plus wing-fuselage interference) of all three wings was approximately the same. The drag due to lift generally decreased with an increase in aspect ratio but generally showed only small variations with Mach number. Increases in aspect ratio produced an increase in maximum lift-drag ratio. Above the drag rise Mach number, all wings exhibited a marked decrease in maximum lift-drag ratio.

INTRODUCTION

A systematic research program is being carried out in the Langley high-speed 7- by 10-foot wind tunnel to determine the aerodynamic characteristics of various arrangements of the component parts of research-type airplane models, including some complete model configurations.

Results are being obtained on characteristics in pitch, yaw, and during steady rolling up to a Mach number of about 0.95. The models are mounted on a sting-type support system. Reynolds numbers range between 1,500,000 and 6,000,000, depending on the wing plan forms and test Mach numbers.

The wing plan forms are similar, in general, to the plan forms investigated at lower Reynolds numbers during a previous research program which utilized the transonic-bump technique for obtaining results at transonic speeds. Some of the results obtained from the transonic-bump program have been summarized in reference 1. Some higher-scale tests of similar or related wing plan forms have been performed in other wind tunnels (references 2 to 4). A comparison of aerodynamic characteristics in pitch as obtained by different test techniques has been reported in reference 5.

The present paper presents results which show the effect of aspect ratio on the pitch characteristics of wings having a sweep angle of 45°, a taper ratio of 0.6, and an NACA 65A006 airfoil section in combination with a fuselage. In order to expedite the issuance of the results, only a limited analysis has been made, although comparisons of some of the more significant characteristics with available theory are presented.

COEFFICIENTS AND SYMBOLS

The symbols used in the present paper are defined in the following list. All forces and moments are presented relative to the quarter chord of the mean aerodynamic chord.

C_L	lift coefficient (Lift/qS)
C_D	drag coefficient (Drag/qS)
C_m	pitching-moment coefficient (Pitching moment/$qS\bar{c}$)
q	dynamic pressure, pounds per square foot ($\rho V^2/2$)
S	wing area, square feet
$\bar{c}$	mean aerodynamic chord (M.A.C.), feet $\left(\frac{2}{S}\int_0^{b/2} c^2\,dy\right)$
c	local wing chord, feet
c_{ave}	average wing chord, feet $\left(\frac{S}{b}\right)$

b	span, feet
ρ	air density, slugs per cubic foot
V	free-stream velocity, feet per second
M	Mach number
R	Reynolds number of wing based on $\bar{c}$
α	angle of attack, degrees
$\Delta\alpha$	local angle-of-attack change due to distortion of wings, degrees
ΔL	lift increment due to distortion of wings, pounds
K	correction factor for C_{L_α} due to wing distortion
C_{L_α}	lift-curve slope $\left(\partial C_L/\partial\alpha\right)$
A	aspect ratio
ΔC_D	drag due to lift $\left(C_D - C_{D_{C_{L=0}}}\right)$
$\Delta\left(\partial C_m/\partial C_L\right)$	incremental change in aerodynamic-center location due to wing distortion
y	spanwise station, feet
$\bar{y}$	spanwise center of pressure (rigid wing), feet
$\bar{y}_{\Delta L}$	spanwise center of pressure of ΔL, feet
$\Lambda_{c/4}$	sweep angle of quarter-chord line, degrees
$c_l c/C_L c_{ave}$	span-load coefficient

Subscripts:

F	fuselage alone
WF	wing-fuselage

MODELS AND APPARATUS

The wing-fuselage combinations investigated are shown in figure 1. All wings had an NACA 65A006 airfoil section parallel to the fuselage center line. A common aluminum fuselage was used, the ordinates of which are shown in table I. The aspect-ratio-2 and -6 wings were constructed of solid aluminum alloy. The aspect-ratio-4 wing was of composite construction, consisting of a steel core and a bismuth-tin covering to give the section contour.

The three wings used in this investigation represent only a part of the family of wings being studied in a more extensive program; therefore, a simplified system for designating the wings (similar to that used in reference 4) is being utilized for this program. For example, the wing designated by 45-4-.6-006 has the quarter-chord line sweptback 45°, an aspect ratio of 4, and a taper ratio of 0.6. The number 006 refers to the section designation; in this case, the design-lift coefficient is zero and the thickness is 6 percent of the chord.

The models were tested on the sting-type support system shown in figure 2. With this support system the model can be remotely operated through a 28° angle range. The internally mounted electrical strain-gage balance used is shown installed in the fuselage in figure 3.

TESTS AND CORRECTIONS

The tests were conducted in the Langley high-speed 7- by 10-foot tunnel through a Mach number range from approximately 0.40 to 0.95. The size of the models used caused the tunnel to choke at corrected Mach numbers of from 0.95 to 0.96, depending on the wing being tested. The blocking corrections which were applied were determined by the velocity-ratio method of reference 6 which utilizes experimental pressures measured at the tunnel wall opposite the model. The corrections determined in this manner were checked by the theoretical method of reference 7 and, in general, good agreement was observed, although above a Mach number of 0.92 the values obtained in reference 7 were somewhat higher.

The jet-boundary corrections which were applied to the lift and drag were calculated by the method of reference 8. The correction to pitching moment was considered negligible.

No tare corrections were obtained; however the results of reference 9 indicate that for a tailless sting-mounted model, similar to the models reported herein, the tare corrections to lift and pitching moment were negligible. The drag data have been corrected to correspond to a

pressure at the base of the fuselage equal to free-stream static pressure. For this correction, the base pressure was determined by measuring the pressure at a point inside the fuselage about 9 inches forward of the base. This correction, which was added to the measured drag coefficient, amounted to a drag coefficient increment that increased from a value of 0.001 to 0.004 for the wing-fuselage configuration and from 0.001 to 0.002 for the fuselage alone, as the Mach number increased from 0.4 to 0.95.

The angle of attack has been corrected for the deflection of the sting-support system under load.

The test wings were known to deflect under load; accordingly, in an effort to correct the measured data to correspond to the rigid case, correction factors for the effect of this aeroelastic distortion were determined. Two types of distortion were considered: (1) The twist of the wing about its elastic axis, and (2) the spanwise change in angle of attack due to bending of the wing under load. Both types of distortion increased markedly with increasing aspect ratio but with 45° sweep the change in angle of attack due to bending is the predominant factor. A preliminary deflection analysis showed practically no deflection of the aspect-ratio-2 wing.

The correction factors for the effects of aeroelastic distortion were determined from static loadings of the wings. In an attempt to approximate this distortion, an elliptical load distribution was simulated by applying loads at four spanwise points along the quarter-chord line of each wing. The change in angle of attack $\Delta\alpha$ (fig. 4) was measured by dial gages at several spanwise stations in the chordwise plane parallel to the fuselage center line. The incremental amount of lift ΔL corresponding to the change in angle of attack was calculated according to strip theory by the equation

$$\Delta L = 2C_{L_\alpha} c_{ave} q \int_0^{b/2} \Delta\alpha \left(\frac{c_l c}{C_L c_{ave}} \right) dy$$

The correction factor K (fig. 5), was determined by the relation $K = (L + \Delta L)/L$ where L is the measured lift.

The correction factor that was derived to account for the change in aerodynamic-center position $\Delta\left(\frac{\partial C_m}{\partial C_L}\right)$ due to aeroelastic distortion is

based on the inboard movement of the lateral center of pressure that results from the reduction in lift due to distortion occurring mostly on the outer portion of the wing. The lateral center of pressure $\bar{y}_{\Delta L}$ of the lift increment ΔL, obtained from the static loadings, was determined from plots of the spanwise distribution of this lift. The correction factor $\Delta\left(\frac{\partial C_m}{\partial C_L}\right)$ was calculated as follows:

$$\Delta\left(\frac{\partial C_m}{\partial C_L}\right) = \left[\frac{\left(\bar{y} - \bar{y}_{\Delta L}\right)}{\bar{c}} \tan \Lambda_{c/4}\right](K - 1)$$

where $\bar{y}$ is the theoretical lateral center of pressure of the rigid wing determined from reference 10. Results from independent calculations using simple beam theory and including the effects of aeroelastic distortion on the span-load distribution are in good agreement with the results obtained from the preceding expressions.

The Reynolds number variation with Mach number for the wings tested is presented in figure 6 and is based on the mean aerodynamic chord of the respective wings.

RESULTS AND DISCUSSION

The results of the investigation are presented in the following figures:

	Figures
Basic data:	
Wing-fuselage	7 to 9
Fuselage alone	10
Summary plots:	
Effects of Mach number	11 to 14
Effects of aspect ratio	15 to 16
Minimum drag	17 to 18
Drag due to lift	19 to 20
Lift-drag ratios	21

Lift Characteristics

No corrections for the effect of aeroelastic distortion have been applied to the basic lift data as presented in figures 7 to 9. Lift-curve slopes measured near zero lift are presented with and without corrections applied in figures 11 to 13. The correction is seen to be of appreciable magnitude for the aspect-ratio-6 wing but is negligible for the aspect-ratio-2 wing.

A comparison of the corrected experimental lift-curve slopes for the wing-fuselage combinations with wing-alone theory (reference 10) indicated good qualitative agreement, although the theory predicts lower magnitude and somewhat smaller effects of Mach number than were obtained experimentally. Previous experience has indicated that the wing-alone theory predicts somewhat smaller effects of Mach number than are obtained by experiment (as examples, see references 3 and 11). These effects also may be due in part to the presence of the fuselage.

The variation of lift-curve slope with aspect ratio, at several Mach numbers, is presented in figure 15, along with a comparison with theory and the experimental data of reference 4. The variation of lift-curve slope with aspect ratio as predicted by the wing-fuselage theory of reference 12 shows good agreement with the experimental data. The wing-alone theory of reference 10 shows good agreement with regard to variation, although, as mentioned before, the absolute magnitudes are somewhat low.

Pitching-Moment Characteristics

The basic pitching-moment data (figs. 7 to 9) have not been corrected for the effects of aeroelastic distortion. The slopes of the pitching-moment curve, measured near zero lift are presented with and without corrections applied in figures 11 to 13. The correction is negligible for the aspect-ratio-2 wing but is large for the aspect-ratio-6 wing.

Below the force-break Mach number the aerodynamic-center location remains relatively constant for all wings (fig. 14); however, above a Mach number of 0.91 the aerodynamic center moves rapidly rearward for all three wings, as would be expected.

The theoretical wing-fuselage aerodynamic-center locations, as predicted by reference 12, are in fairly good agreement with the experimental results (fig. 16). The small discrepancies shown may be due in part to the fact that the effect of the presence of the fuselage on the theoretical span-load distributions, which are obtained from reference 10, is not considered in the theory of reference 12. It will also be noted that at the highest aspect ratios, the wing-alone theory of reference 10,

which reference 12 uses as a basis, is in poor agreement with the wing-alone data of reference 4 (fig. 16, M = 0.40).

At the higher lift coefficients the pitching-moment curves of the aspect-ratio-4 and 6 wings (figs. 8 and 9) indicate destabilizing breaks, with the break for the aspect-ratio-6 wing being more severe and occurring at a lower lift coefficient than that of the aspect-ratio-4 wing. The wing of aspect ratio 2 exhibits a definite stabilizing trend at the higher lift coefficients. These effects are in agreement with the correlation presented in reference 13.

Drag Characteristics

Drag at zero lift.- At Mach numbers below the force break there is some variation in minimum drag coefficient between the three wing-fuselage configurations (fig. 14). Inasmuch as a common fuselage was used and the wing area of the three wings varied with aspect ratio, the increment of drag coefficient attributable directly to the fuselage also varied as shown in figure 17. To give a better comparison of minimum drag coefficients, the wing plus wing-fuselage interference drag is plotted in figure 18. The wing plus wing-fuselage interference drag was obtained by subtracting the fuselage-alone drag (fig. 17) from the wing-fuselage drag of figure 14. The slight difference shown can be attributed partly to interference effects and partly to the relative accuracy of the results. The drag-rise Mach number tended to increase slightly with increase in aspect ratio (fig. 18); this same effect has been noted in reference 14.

Drag due to lift.- At the lower lift coefficients the drag due to lift decreased with an increase in aspect ratio (fig. 19) as would be expected. The drag due to lift of the aspect-ratio-2 and 4 wings is not affected by Mach number (fig. 20), but the drag coefficient of the aspect-ratio-6 wing decreased at the higher Mach numbers. The data of reference 1 show the same trend for this wing. The reason for this reduction is not understood but it can possibly be attributed to the washout of the wing due to distortion. Figure 20 also presents a comparison with the theoretical values $\left(\text{given approximately by } C_L^2/\pi A\right)$ for the condition of the resultant force normal to the local relative wind. It will be noted that the experimental drag due to lift breaks away from the theoretical curve at a low lift coefficient, indicating the possibility of an early loss of leading-edge suction because of leading-edge separation.

Lift-Drag Ratios

The results shown in figure 14 indicate that Mach number has little effect on the maximum lift-drag ratio up to the drag-rise Mach number, but above this point a rapid decrease occurs. The maximum lift-drag ratios increase with increasing aspect ratio, as expected. However, due to lower minimum drag, the aspect-ratio-2 wing-fuselage combination has a maximum lift-drag ratio about as high as that of the aspect-ratio-4 wing-fuselage combination. It will also be noted (fig. 21) that at high lift coefficients a very substantial gain in lift-drag ratio is obtained with increasing aspect ratio at the higher Mach numbers. Reduction in aspect ratio is seen to reduce the lift coefficients at which the maximum lift-drag ratio occurs (fig. 21).

CONCLUSIONS

The results of the investigation of the effect of aspect ratio and Mach number on the aerodynamic characteristics in pitch of 45° sweptback wings with 0.6 taper ratio and an NACA 65A006 airfoil section indicated the following conclusions:

1. The variation with Mach number of the lift-curve slope, as predicted by wing-alone theory, was in good qualitative agreement with the experimental results, although the absolute magnitudes were somewhat low. The theoretical lift-curve-slope variation with aspect ratio, as predicted by wing-fuselage theory, was in good agreement with experiment at a low Mach number for which the comparison was made.

2. The theoretical wing-fuselage aerodynamic-center variation with aspect ratio, as predicted by wing-fuselage theory, shows fair agreement with the experimental results. The experimental aerodynamic center showed little variation with Mach number up to the force break; however, above the force-break Mach numbers all wing-fuselage combinations exhibited rapid rearward movements of the aerodynamic center.

3. The zero-lift drag (wing plus wing-fuselage interference) of all three wings was approximately the same at Mach numbers below the drag rise. The drag-rise Mach number tended to increase slightly with increase in aspect ratio.

4. The drag due to lift generally decreased with an increase in aspect ratio and showed only small variations with Mach number within the range of these tests.

5. The maximum lift-drag ratio increased with increase in aspect ratio. All wings exhibited a marked decrease in maximum lift-drag ratio above the drag-rise Mach number.

Langley Aeronautical Laboratory
National Advisory Committee for Aeronautics
Langley Field, Va.

REFERENCES

1. Polhamus, Edward C.: Summary of Results Obtained by Transonic-Bump Method on Effects of Plan Form and Thickness on Lift and Drag Characteristics of Wings at Transonic Speeds. NACA RM L51H30, 1951.

2. Luoma, Arvo A.: Aerodynamic Characteristics of Four Wings of Sweepback Angles 0°, 35°, 45°, and 60°, NACA 65A006 Airfoil Section, Aspect Ratio 4, and Taper Ratio 0.6 in Combination with a Fuselage at High Subsonic Mach Numbers and at a Mach Number of 1.2. NACA RM L51D13, 1951.

3. Sutton, Fred B., and Martin Andrew: Aerodynamic Characteristics Including Pressure Distributions of a Fuselage and Three Combinations of the Fuselage with Sweptback Wings at High Subsonic Speeds. NACA RM A50J26a, 1951.

4. Cahill, Jones F., and Gottlieb, Stanley M.: Low-Speed Aerodynamic Characteristics of a Series of Swept Wings Having NACA 65A006 Airfoil Sections. NACA RM L50F16, 1950.

5. Donlan, Charles J., Myers, Boyd C. II, and Mattson, Axel T.: A Comparison of the Aerodynamic Characteristics at Transonic Speeds of Four Wing-Fuselage Configurations as Determined from Different Test Techniques. NACA RM L50H02, 1950.

6. Hensel, Rudolf W.: Rectangular-Wind-Tunnel Blocking Corrections Using the Velocity-Ratio Method. NACA TN 2372, 1951.

7. Herriot, John G.: Blockage Corrections for Three-Dimensional-Flow Closed-Throat Wind Tunnels, with Consideration of the Effect of Compressibility. NACA Rep. 995, 1950. (Supersedes NACA RM A7B28.)

8. Gillis, Clarence L., Polhamus, Edward C., and Gray, Joseph L., Jr.: Charts for Determining Jet-Boundary Corrections for Complete Models in 7- by 10-Foot Closed Rectangular Wind Tunnels. NACA ARR L5G31, 1945.

9. Osborne, Robert S.: High-Speed Wind-Tunnel Investigation of the Longitudinal Stability and Control Characteristics of a $\frac{1}{16}$-Scale Model of the D-558-2 Research Airplane at High Subsonic Mach Numbers and at a Mach Number of 1.2. NACA RM L9C04, 1949.

10. DeYoung, John: Theoretical Additional Span Loading Characteristics of Wings with Arbitrary Sweep, Aspect Ratio, and Taper Ratio. NACA TN 1491, 1947.

11. Murray, Harry E.: Comparison with Experiment of Several Methods of Predicting the Lift of Wings in Subsonic Compressible Flow. NACA TN 1739, 1948.

12. McLaughlin, Milton D.: Method of Estimating the Stick-Fixed Longitudinal Stability of Wing-Fuselage Configurations Having Unswept or Swept Wings. NACA RM L51J23, 1952.

13. Shortal, Joseph A., and Maggin, Bernard: Effect of Sweepback and Aspect Ratio on Longitudinal Stability Characteristics of Wings at Low Speeds. NACA TN 1093, 1946.

14. Polhamus, Edward C., and King, Thomas J., Jr.: Aerodynamic Characteristics of Tapered Wings Having Aspect Ratios of 4, 6, and 8, Quarter-Chord Lines Swept Back 45°, and NACA 65_1A012 Airfoil Sections. Transonic-Bump Method. NACA RM L51C26, 1951.

TABLE I

FUSELAGE ORDINATES

[Basic fineness ratio 12, actual fineness ratio 9.8 achieved by cutting off rear portion of body]

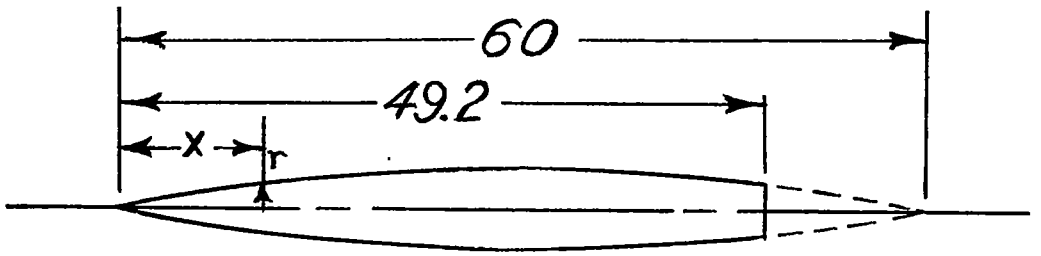

Ordinates (in.)	
x	r
0	0
.30	.139
.45	.179
.75	.257
1.50	.433
3.00	.723
4.50	.968
6.00	1.183
9.00	1.556
12.00	1.854
15.00	2.079
18.00	2.245
21.00	2.360
24.00	2.438
27.00	2.486
30.00	2.500
33.00	2.478
36.00	2.414
39.00	2.305
42.00	2.137
49.20	1.650
L.E. radius = 0.030 inch	

Fuselage

Length	49.2 in.
Max. dia.	5.0 in.
Position of max. dia. (from nose of model)	30.0 in

Sweep angle	45°
Taper ratio	.6
Incidence	0
Dihedral	0
Airfoil section parallel to fuselage ℄	NACA 65A006

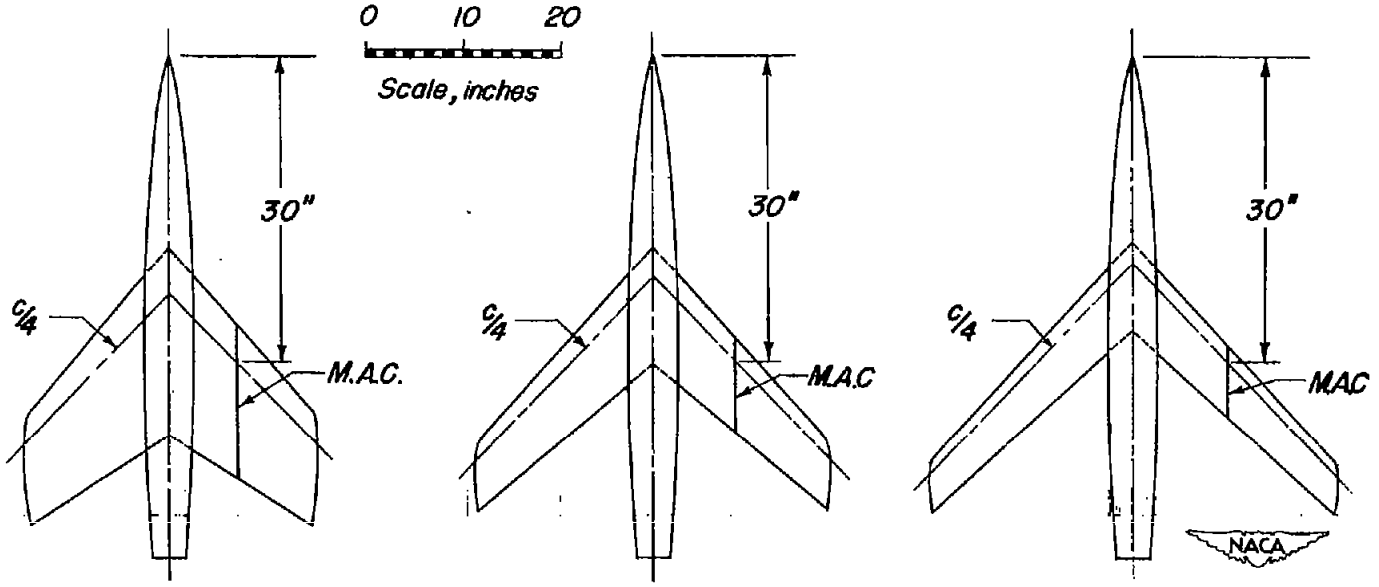

Wing 45-2-0.6-006	
Aspect ratio	2
Area	3.00 sq ft
Span	2.45 ft
Root chord	18.36 in.
Tip chord	11.02 in.
Mean aerodynamic chord	1.250 ft

Wing 45-4-0.6-006	
Aspect ratio	4
Area	2.25 sq ft
Span	3.00 ft
Root chord	11.25 in.
Tip chord	6.75 in.
Mean aerodynamic chord	0.765 ft

Wing 45-6-0.6-006	
Aspect ratio	6
Area	2.00 sq ft
Span	3.46 ft
Root chord	7.22 in.
Tip chord	4.34 in.
Mean aerodynamic chord	0.488 ft

Figure 1.- Drawing of the three wing-fuselage configurations.

Figure 2.- Photograph of a model installed on the variable angle sting support used in the Langley high-speed 7- by 10-foot tunnel.

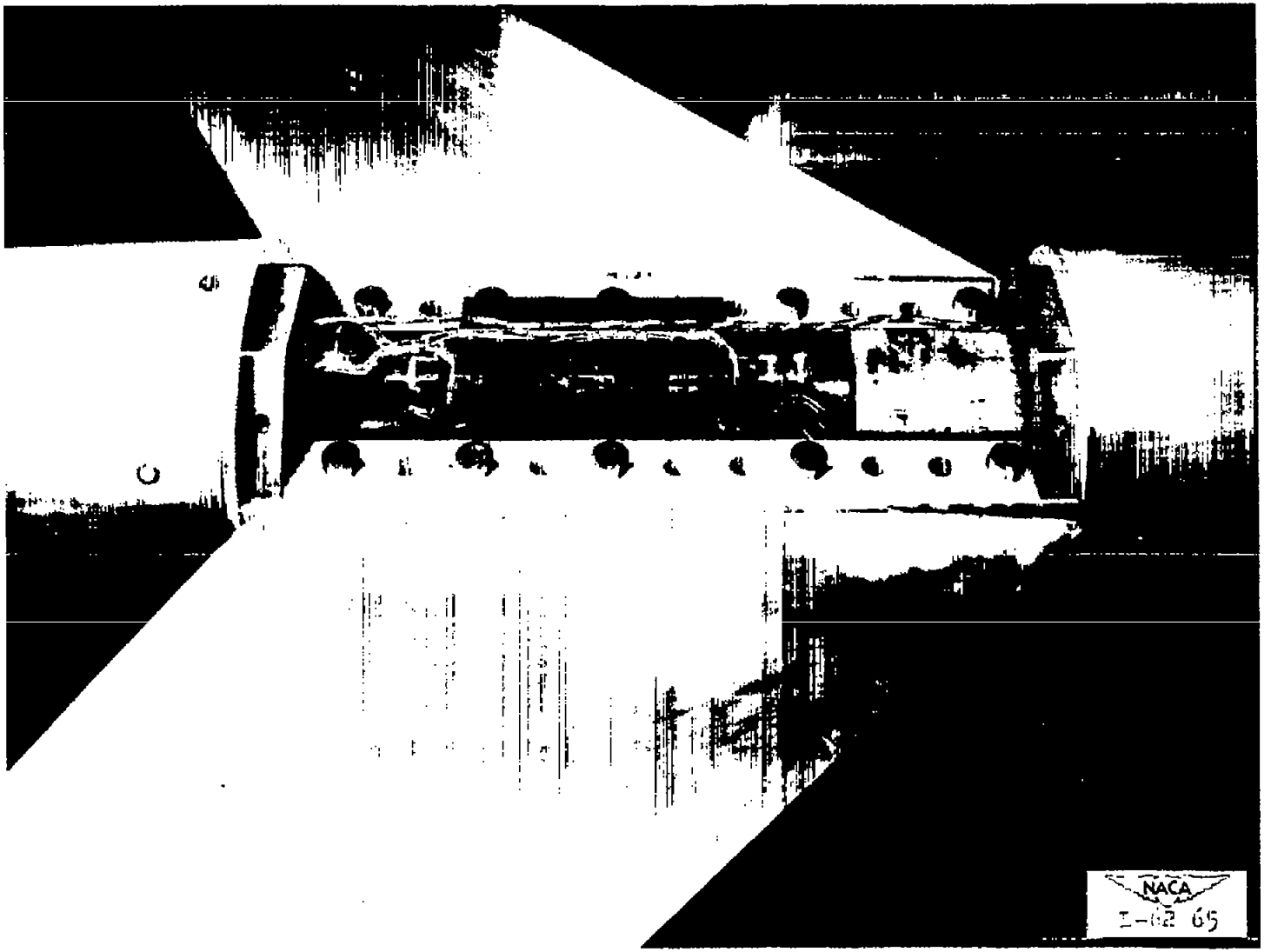

Figure 3.- Photograph of a model showing details of construction and the strain-gage balance.

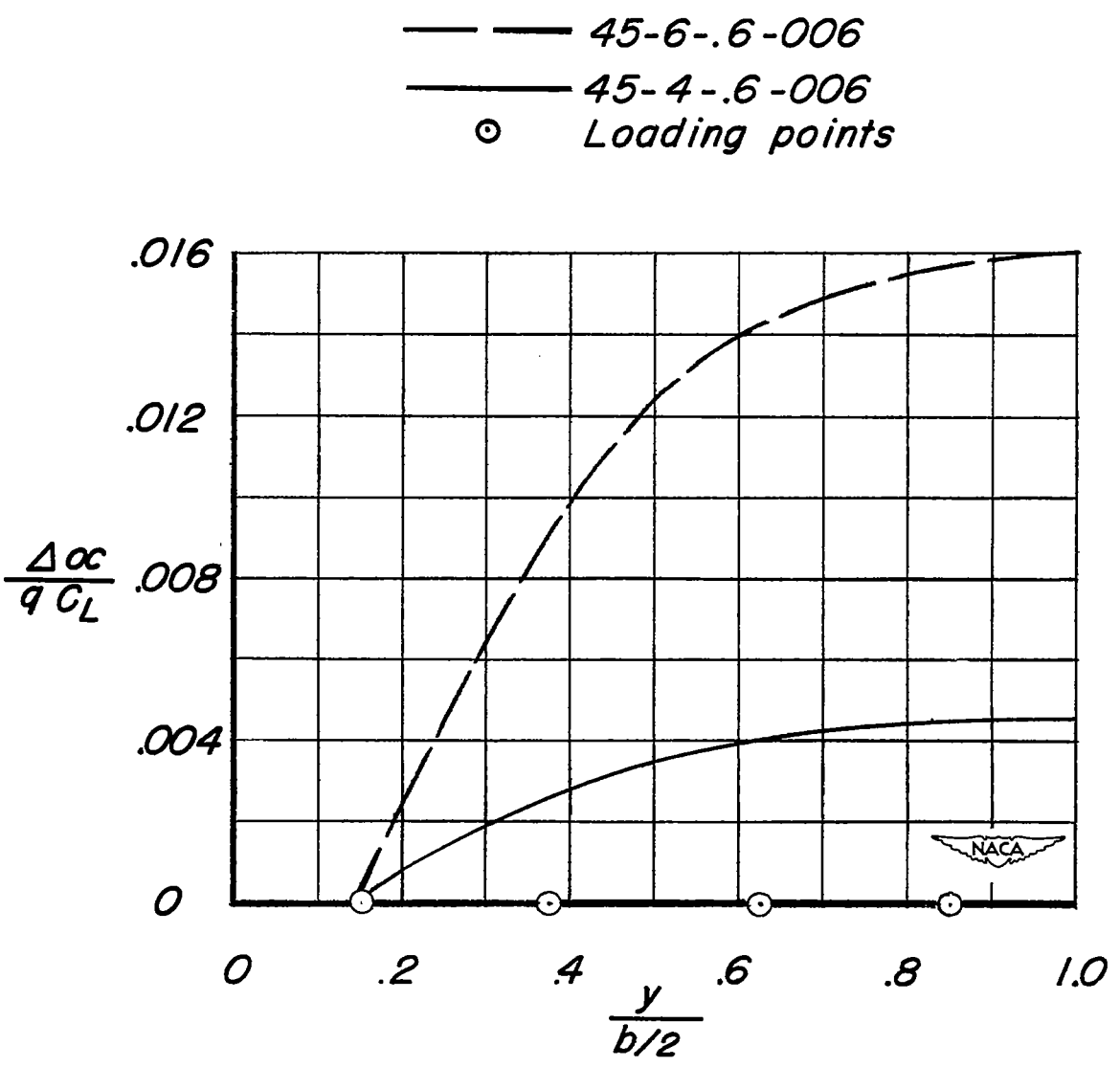

Figure 4.- Spanwise variation of angle of attack due to aeroelastic distortion.

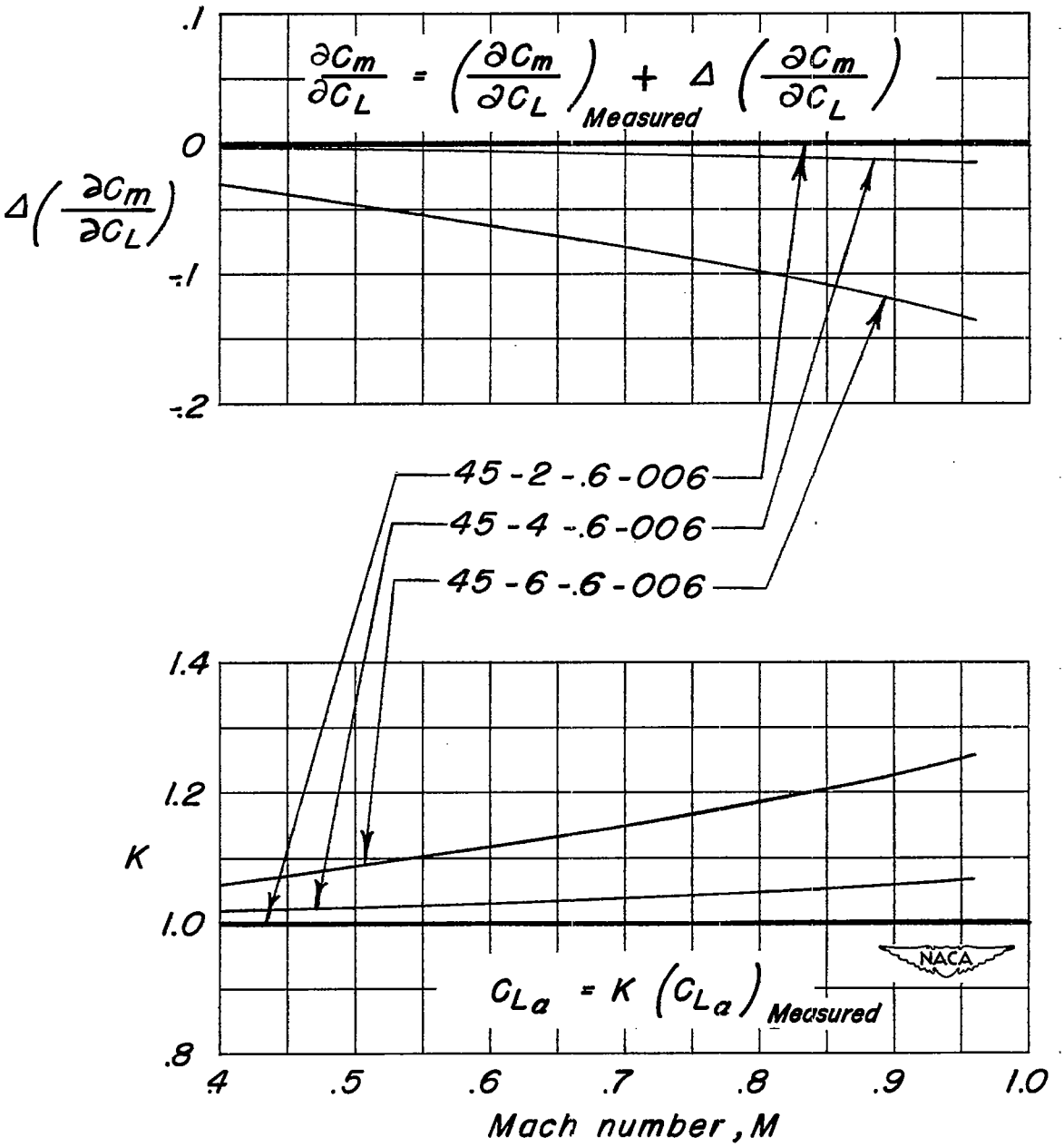

Figure 5.- Correction factors used to correct the summary data for the effects of aeroelastic distortion.

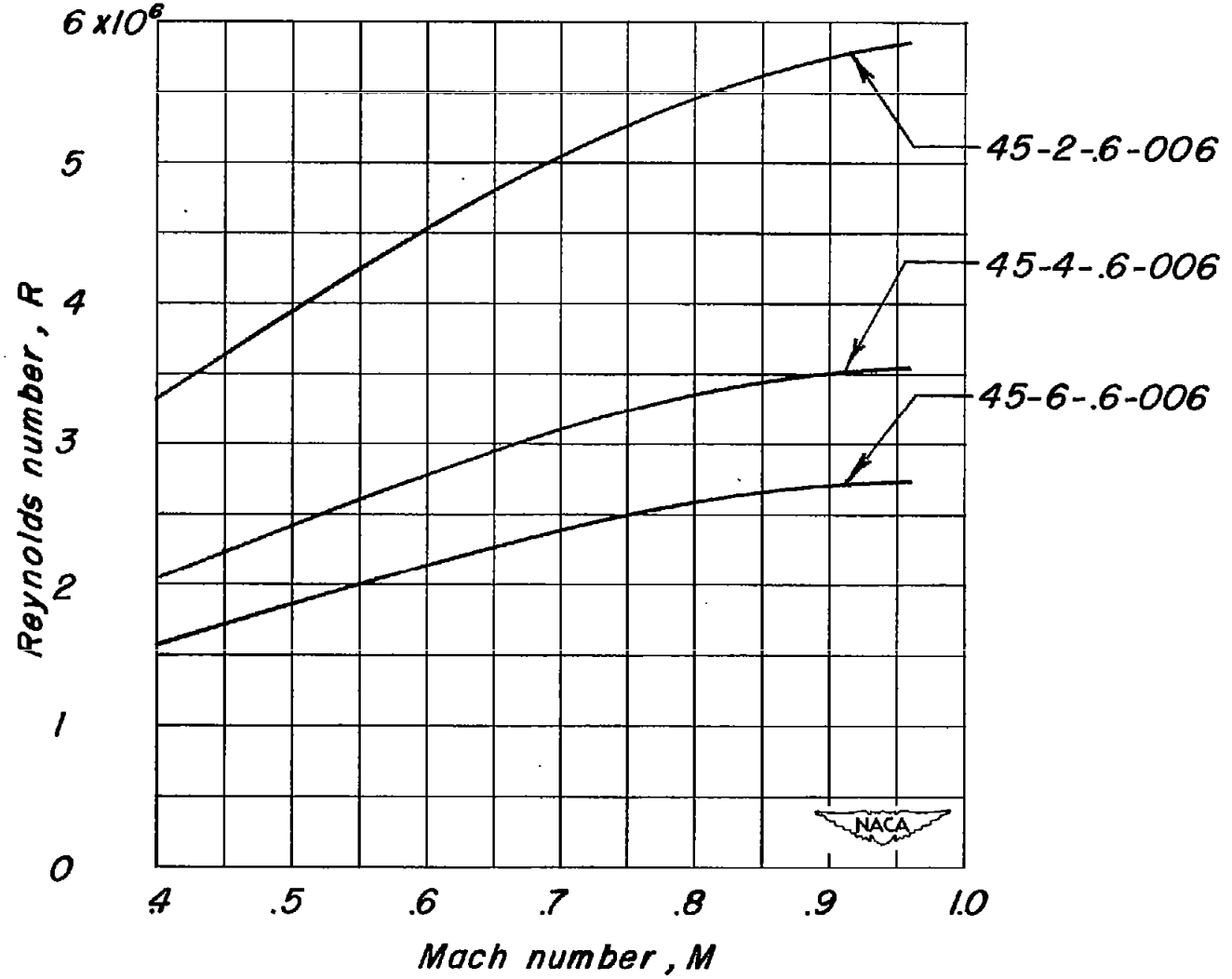

Figure 6.- Variation of Reynolds number with Mach number based on the mean aerodynamic chord.

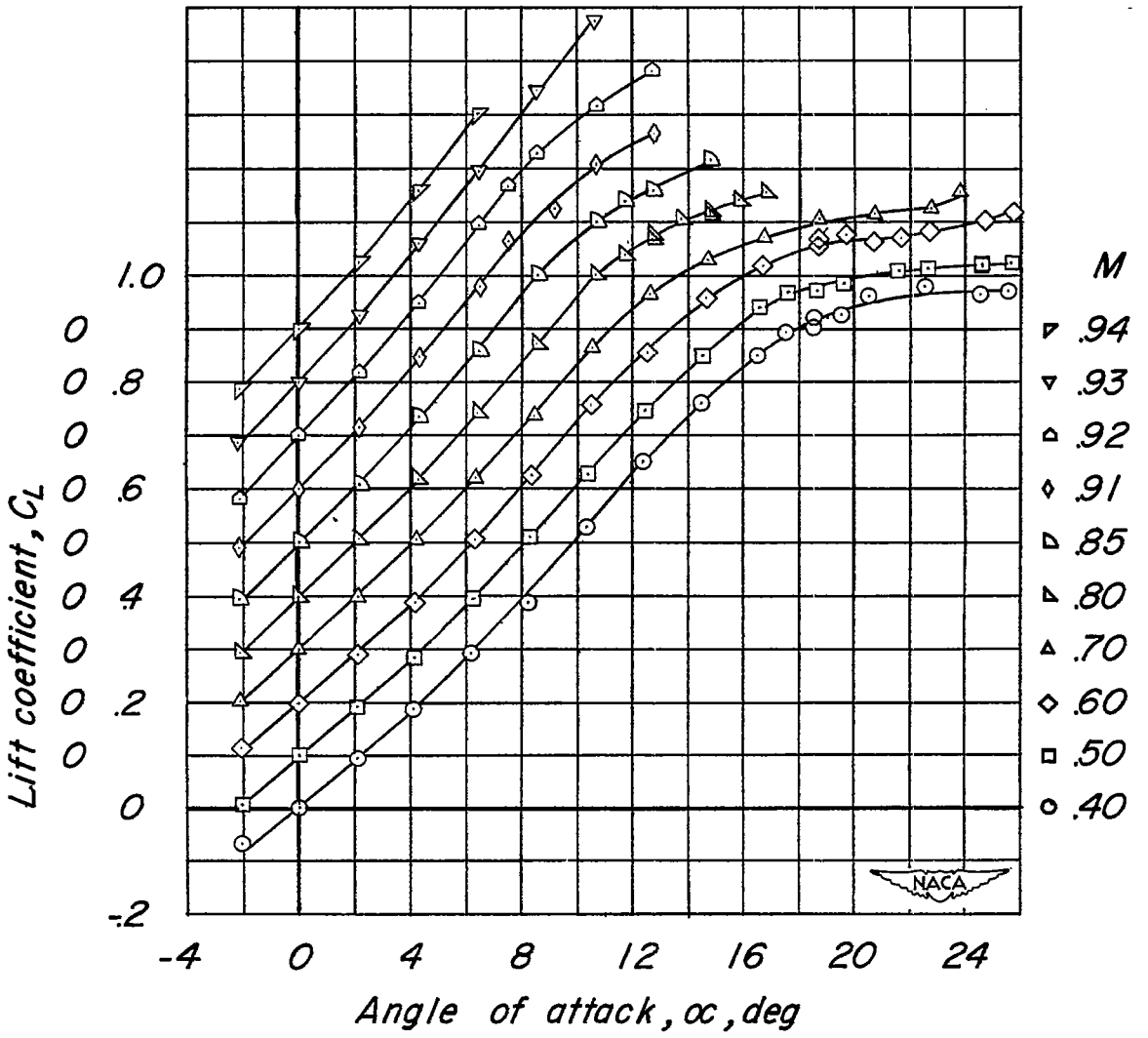

(a) Lift (45-2-.6-006).

Figure 7.- Aerodynamic characteristics of the aspect-ratio-2 wing-fuselage configuration. Not corrected for aeroelastic distortion.

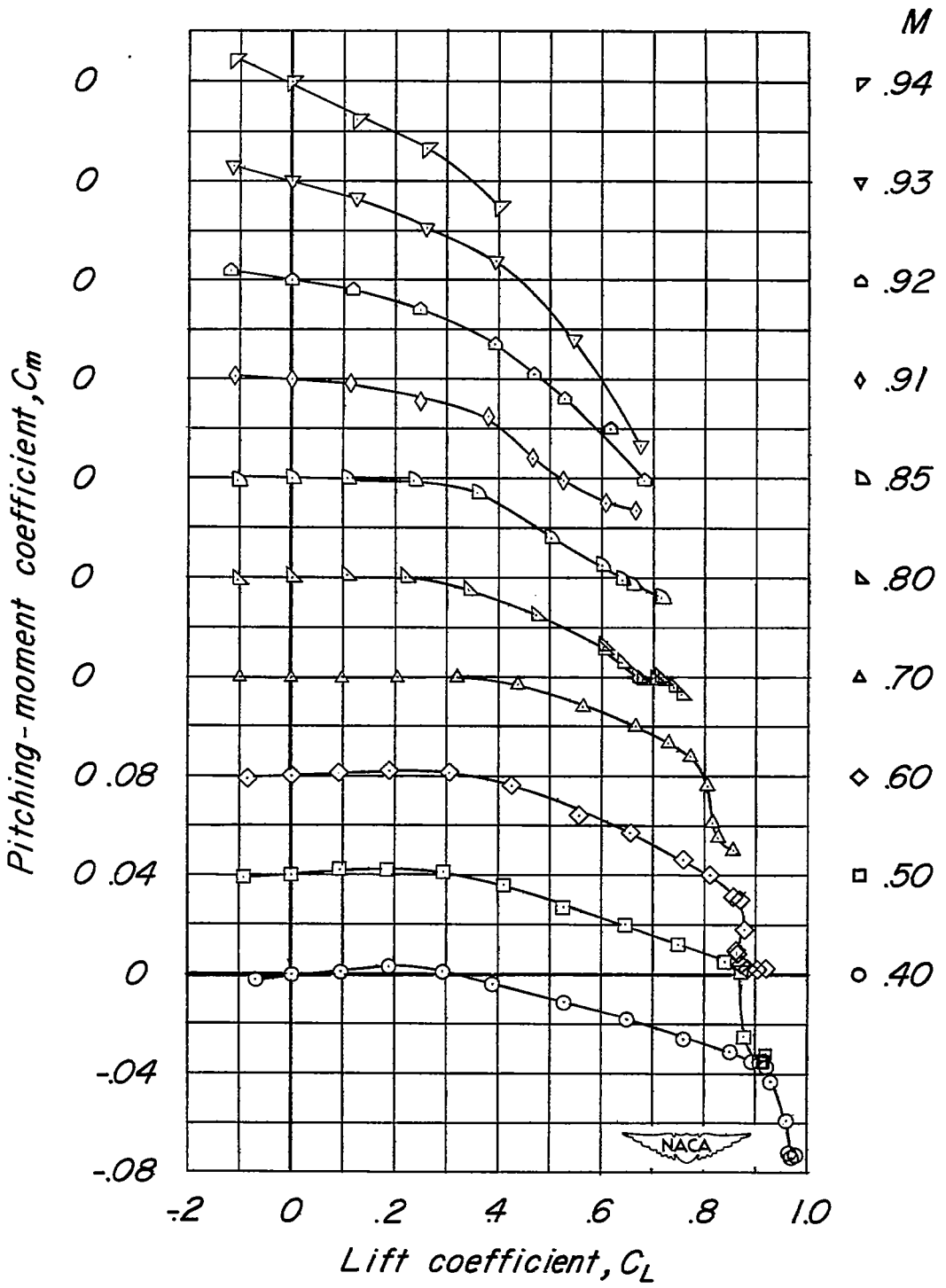

(b) Pitching moment (45-2-.6-006).

Figure 7.- Continued.

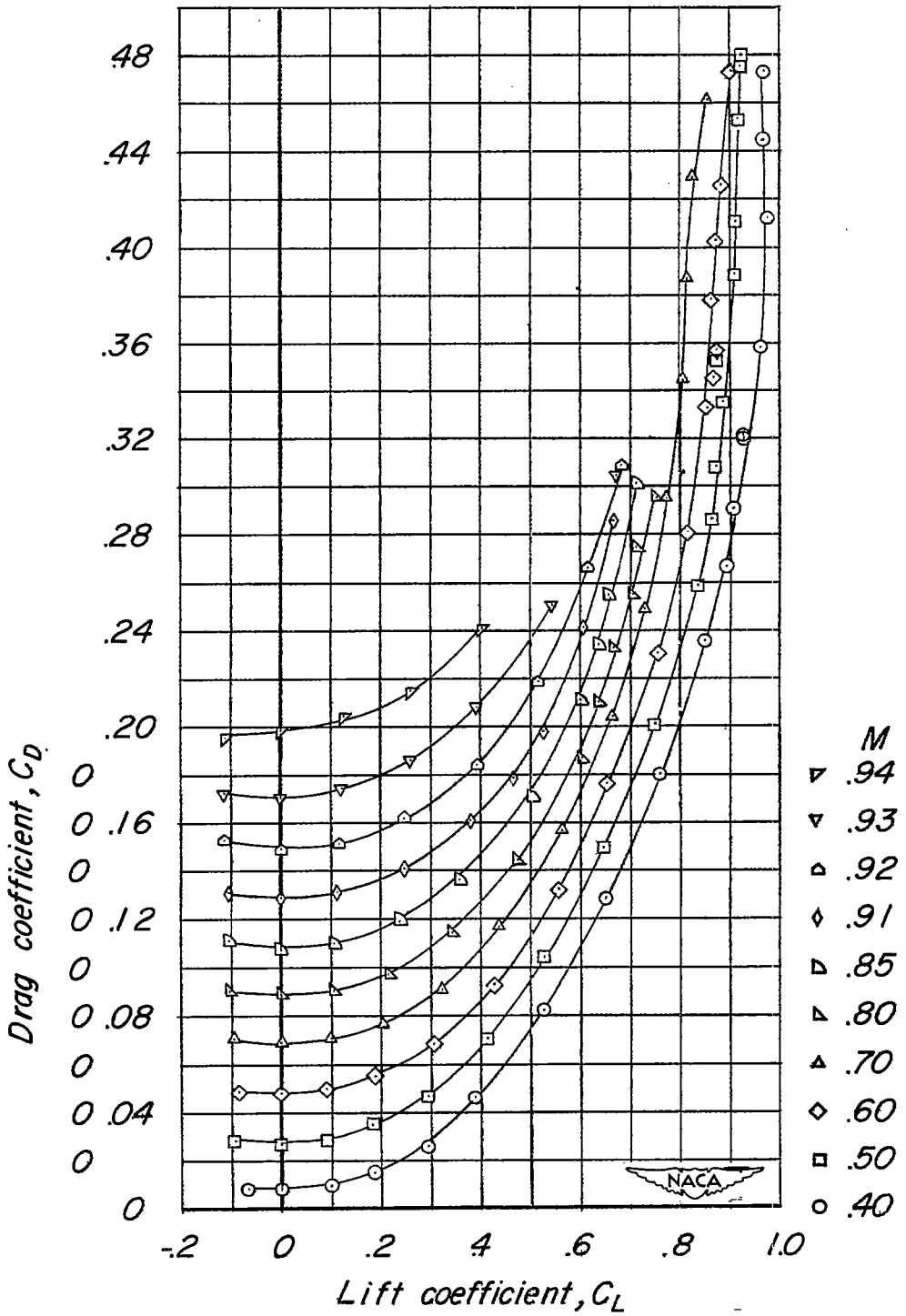

(c) Drag (45-2-.6-006).

Figure 7.- Continued.

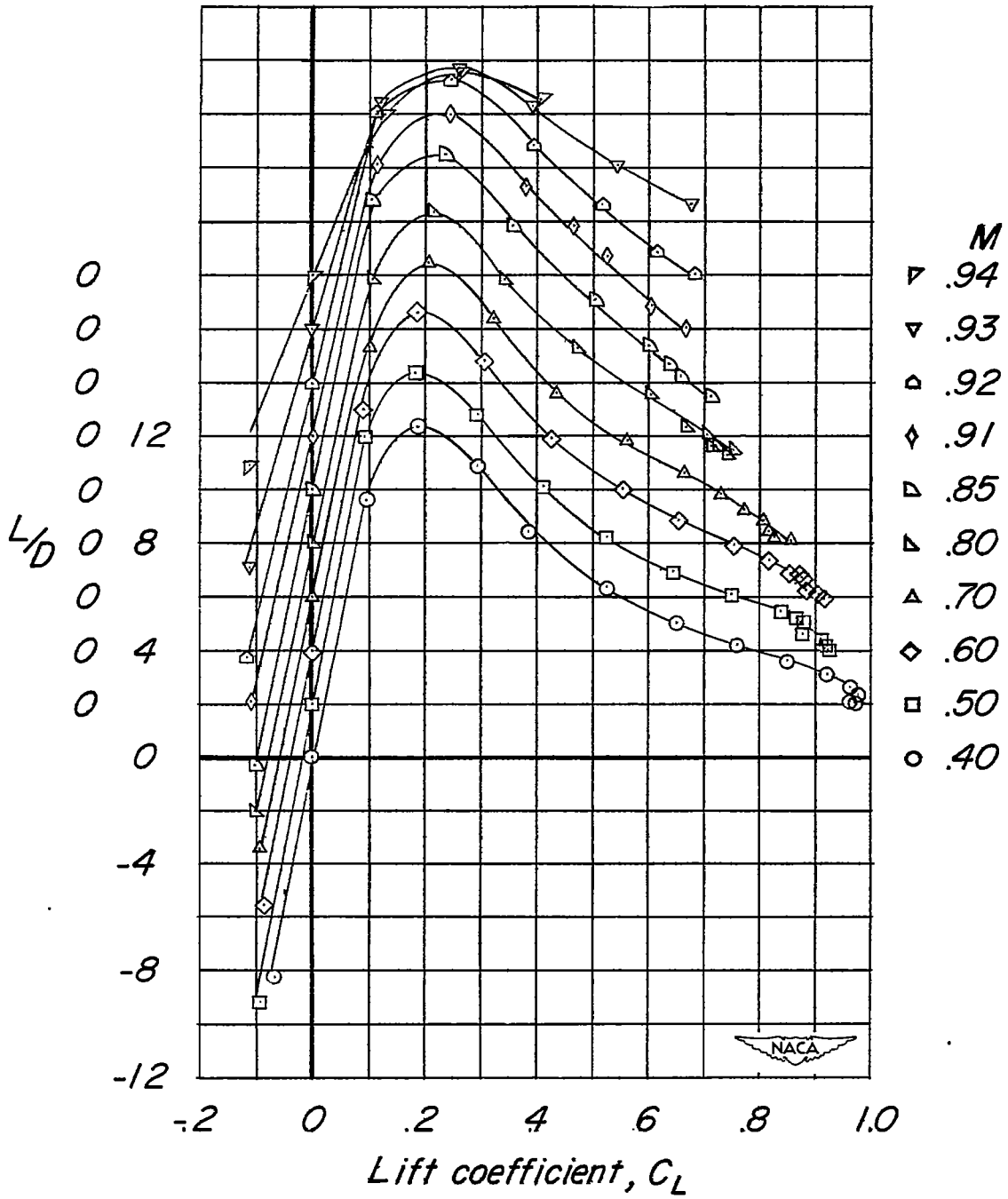

(d) Lift-drag ratios (45-2-.6-006).

Figure 7.- Concluded.

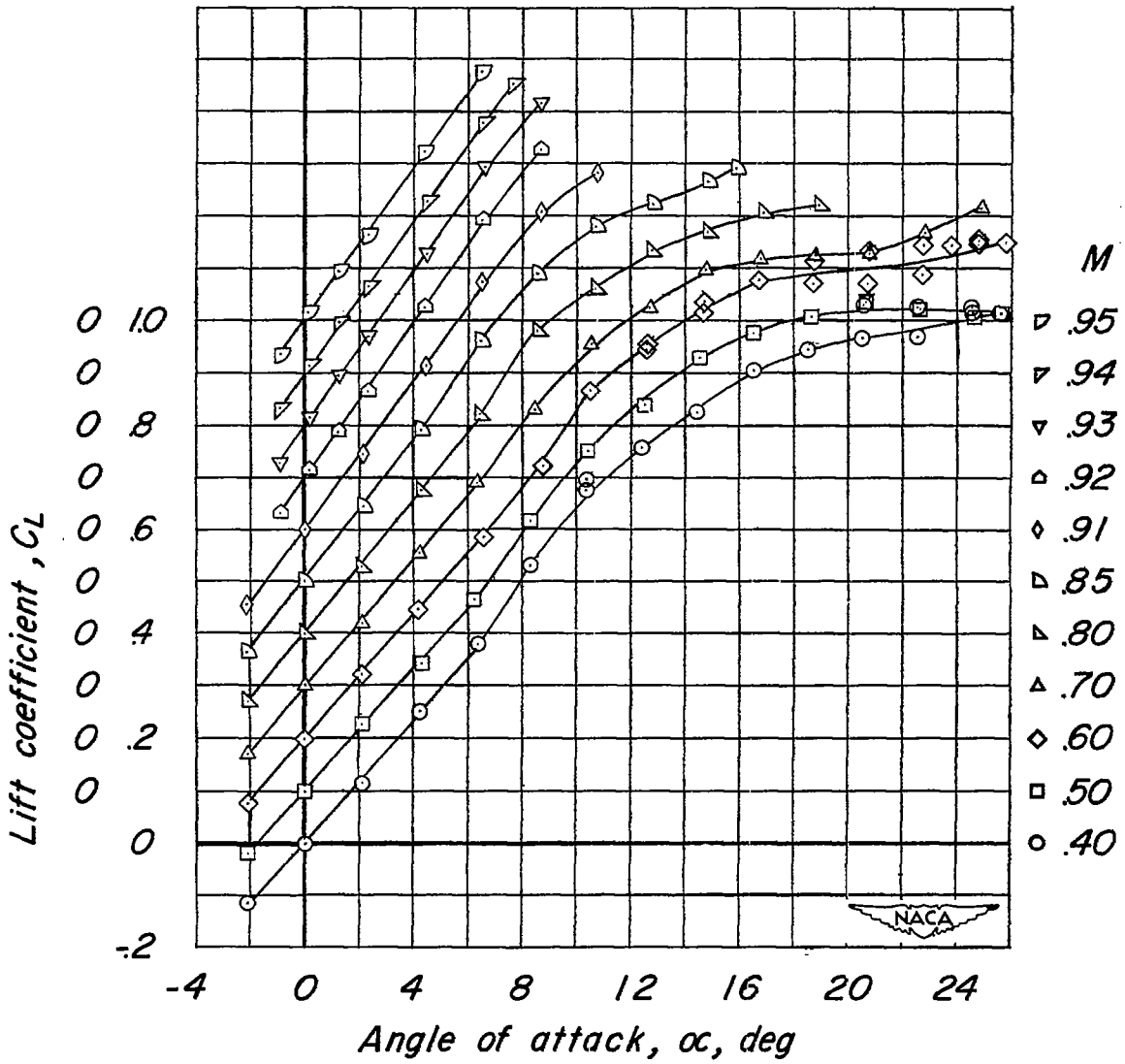

(a) Lift (45-4-.6-006).

Figure 8.- Aerodynamic characteristics of the aspect-ratio-4 wing-fuselage configuration. Not corrected for aeroelastic distortion.

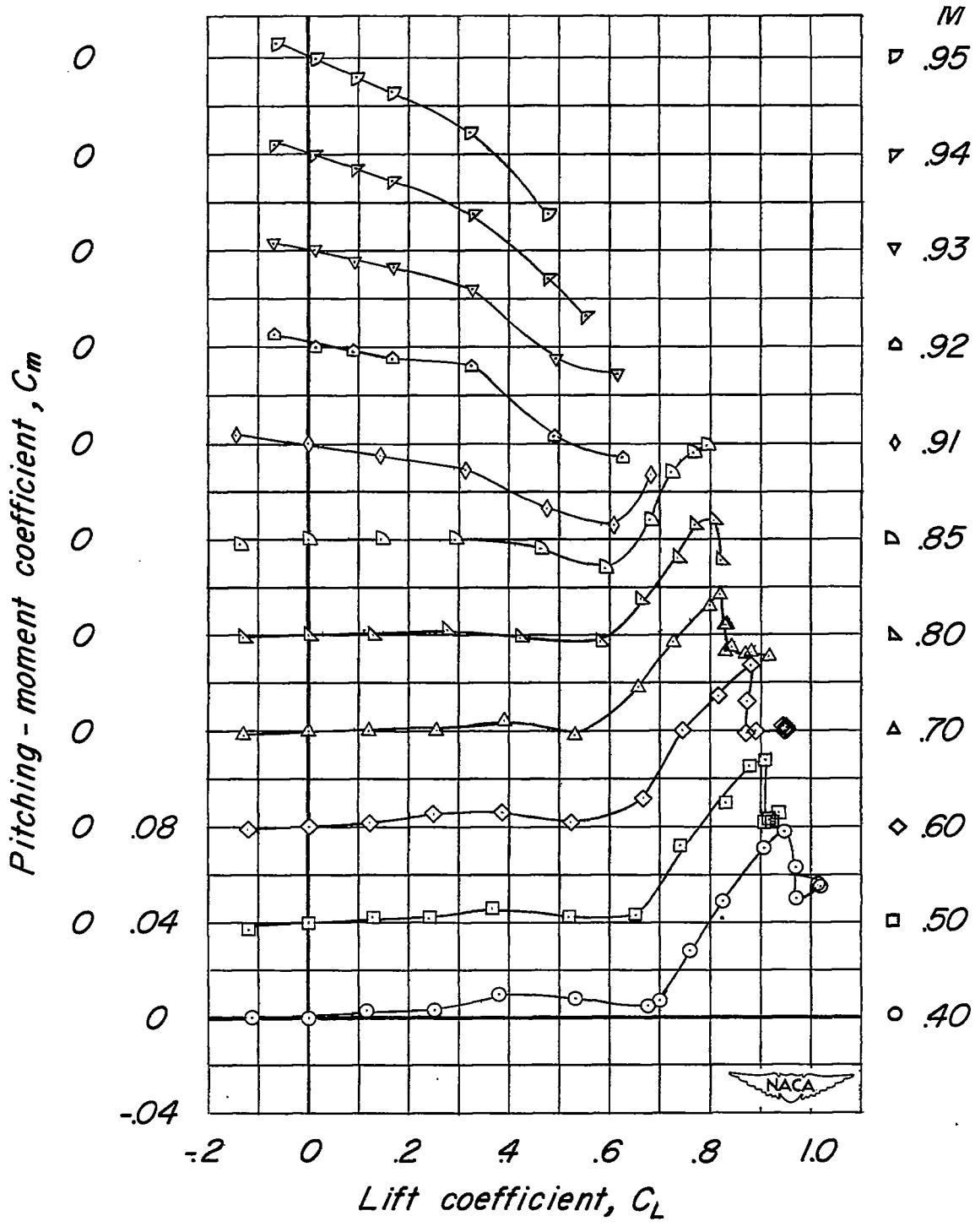

(b) Pitching moment (45-4-.6-006).

Figure 8.- Continued.

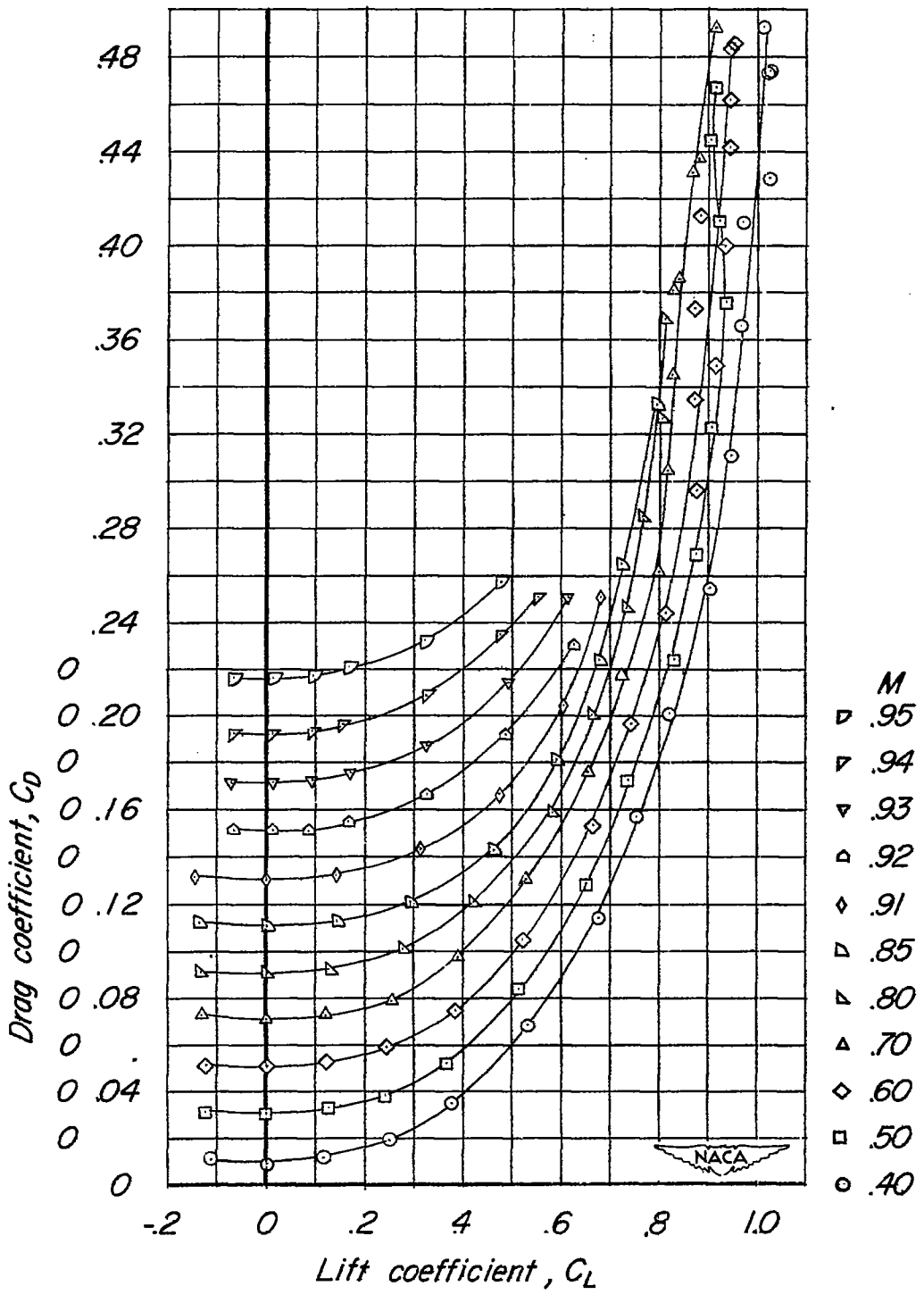

(c) Drag (45-4-.6-006).

Figure 8.- Continued.

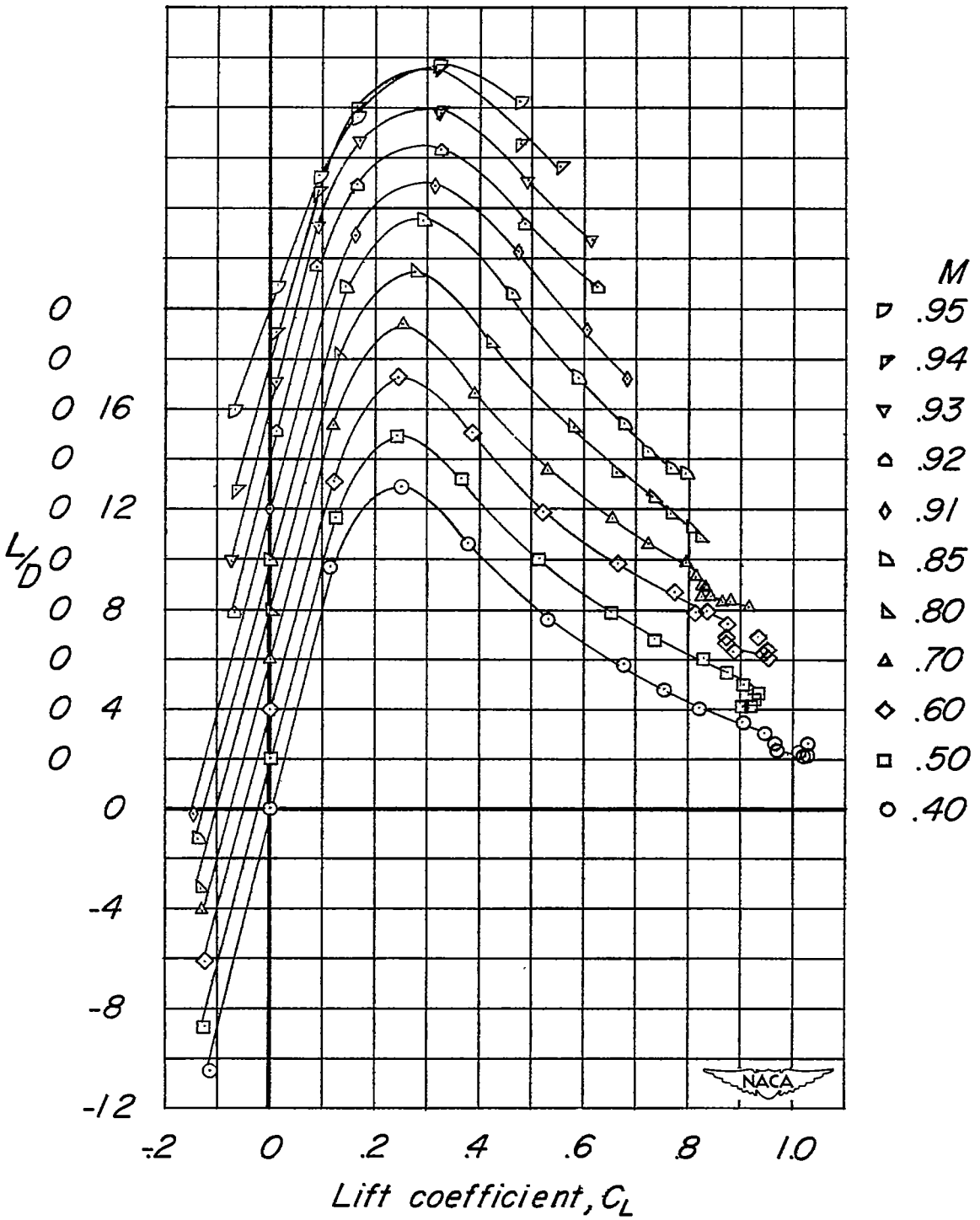

(d) Lift-drag ratios (45-4-.6-006).

Figure 8.- Concluded.

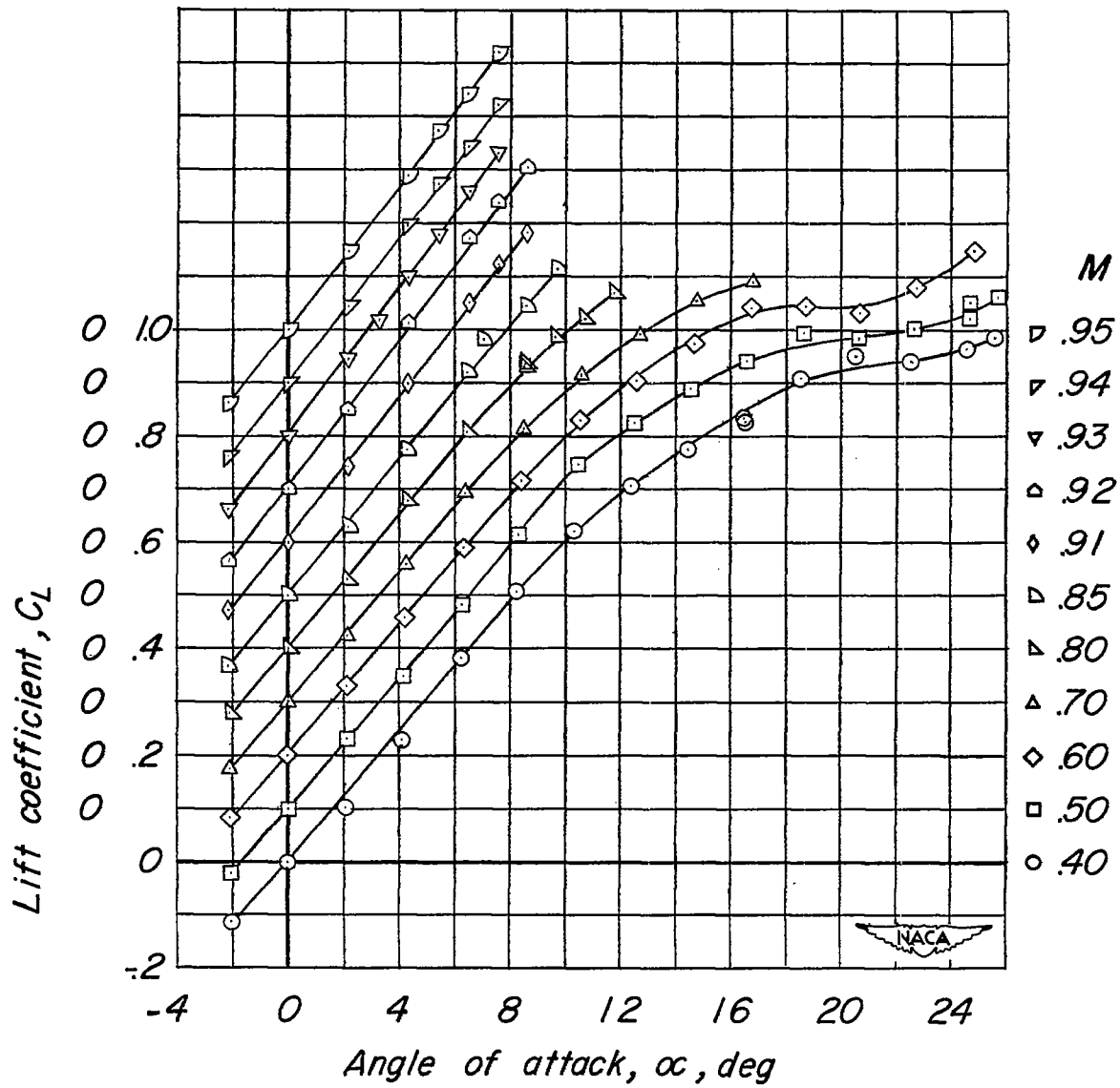

(a) Lift (45-6-.6-006).

Figure 9.- Aerodynamic characteristics of the aspect-ratio-6 wing-fuselage configuration. Not corrected for aeroelastic distortion.

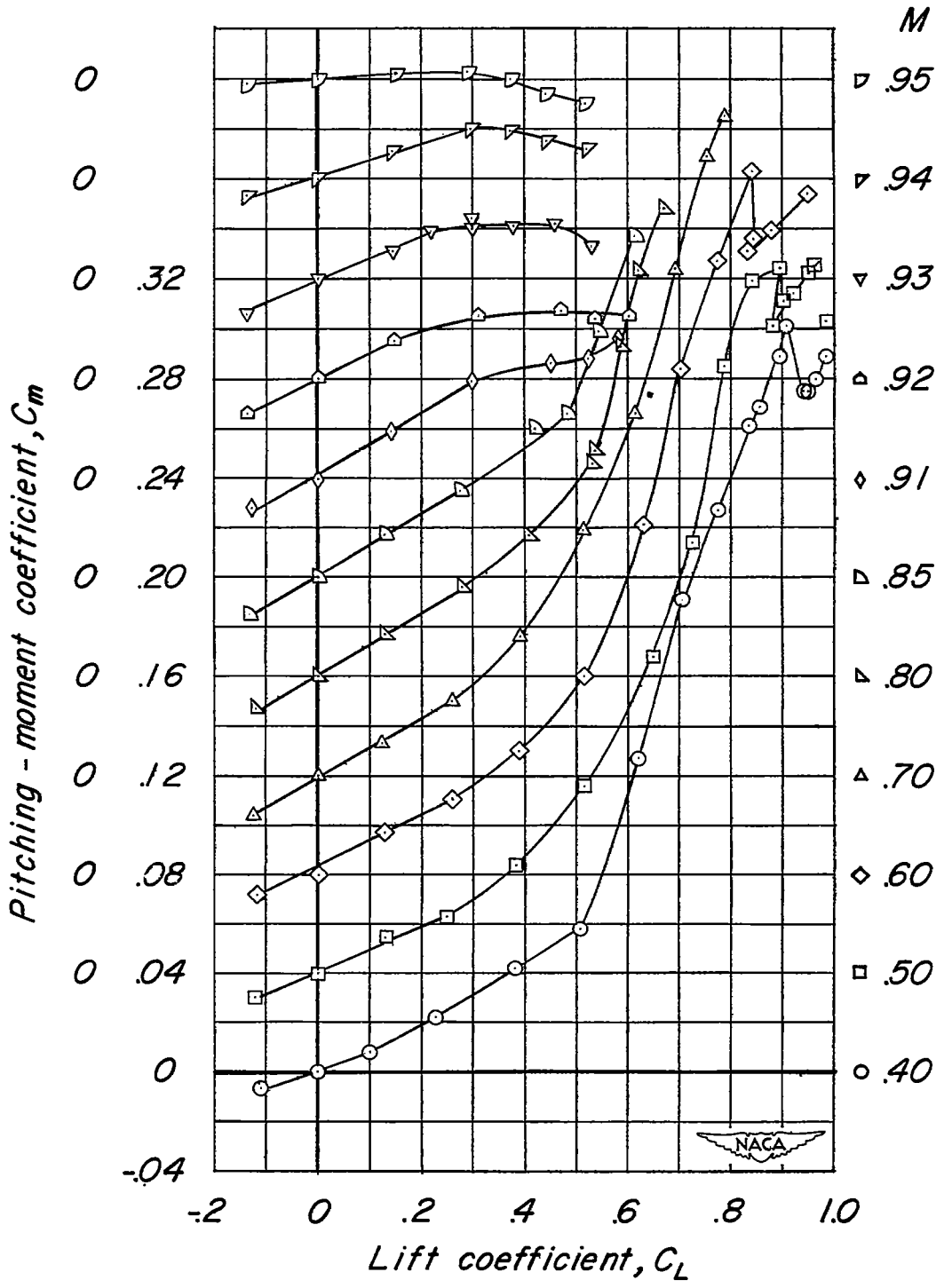

(b) Pitching moment (45-6-.6-006).

Figure 9.- Continued.

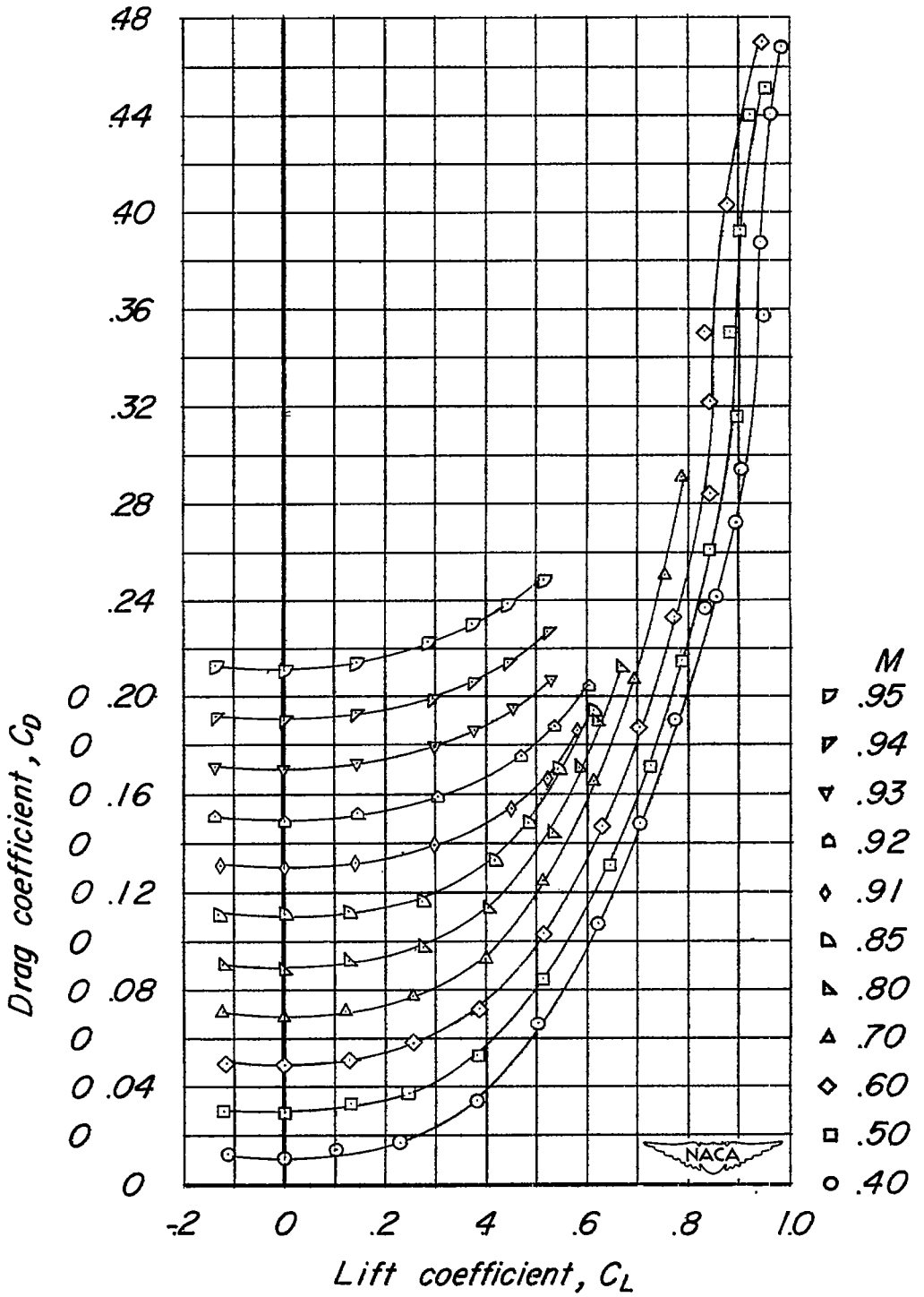

(c) Drag (45-6-.6-006).

Figure 9.- Continued.

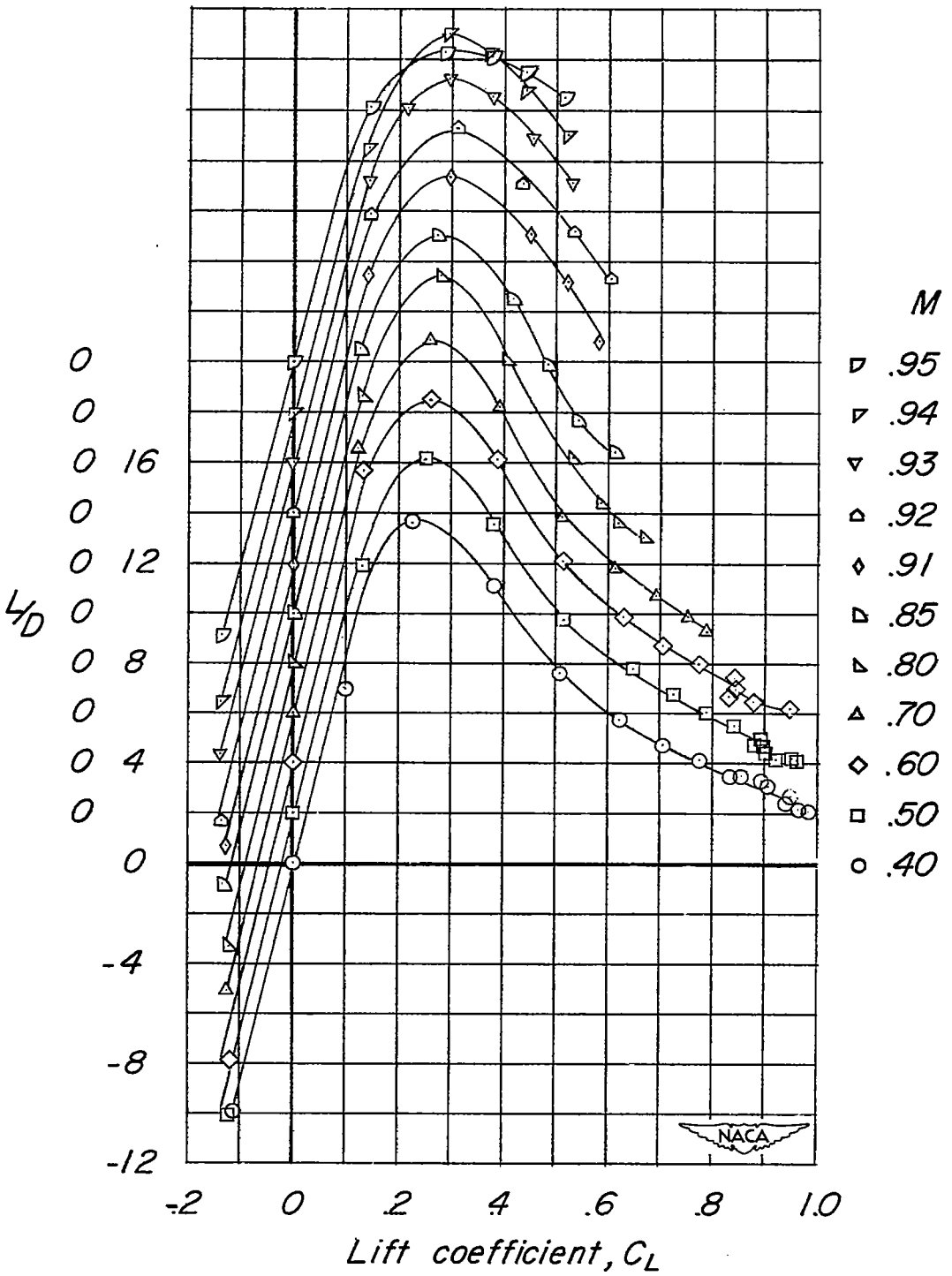

(d) Lift-drag ratios (45-6-.6-006).

Figure 9.- Concluded.

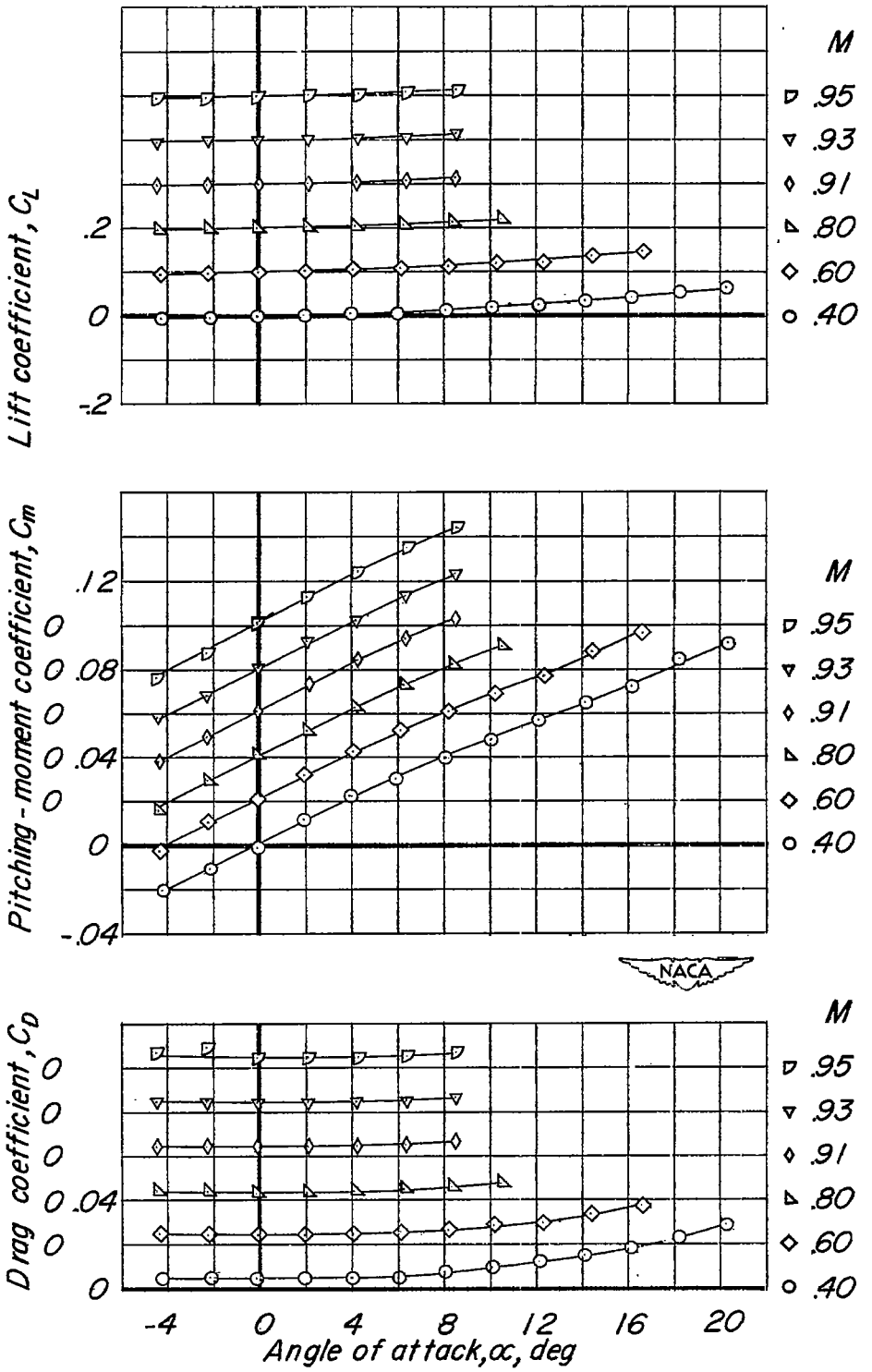

Figure 10.- Aerodynamic characteristics of the fuselage alone. Coefficients based on the aspect-ratio-4 wing.

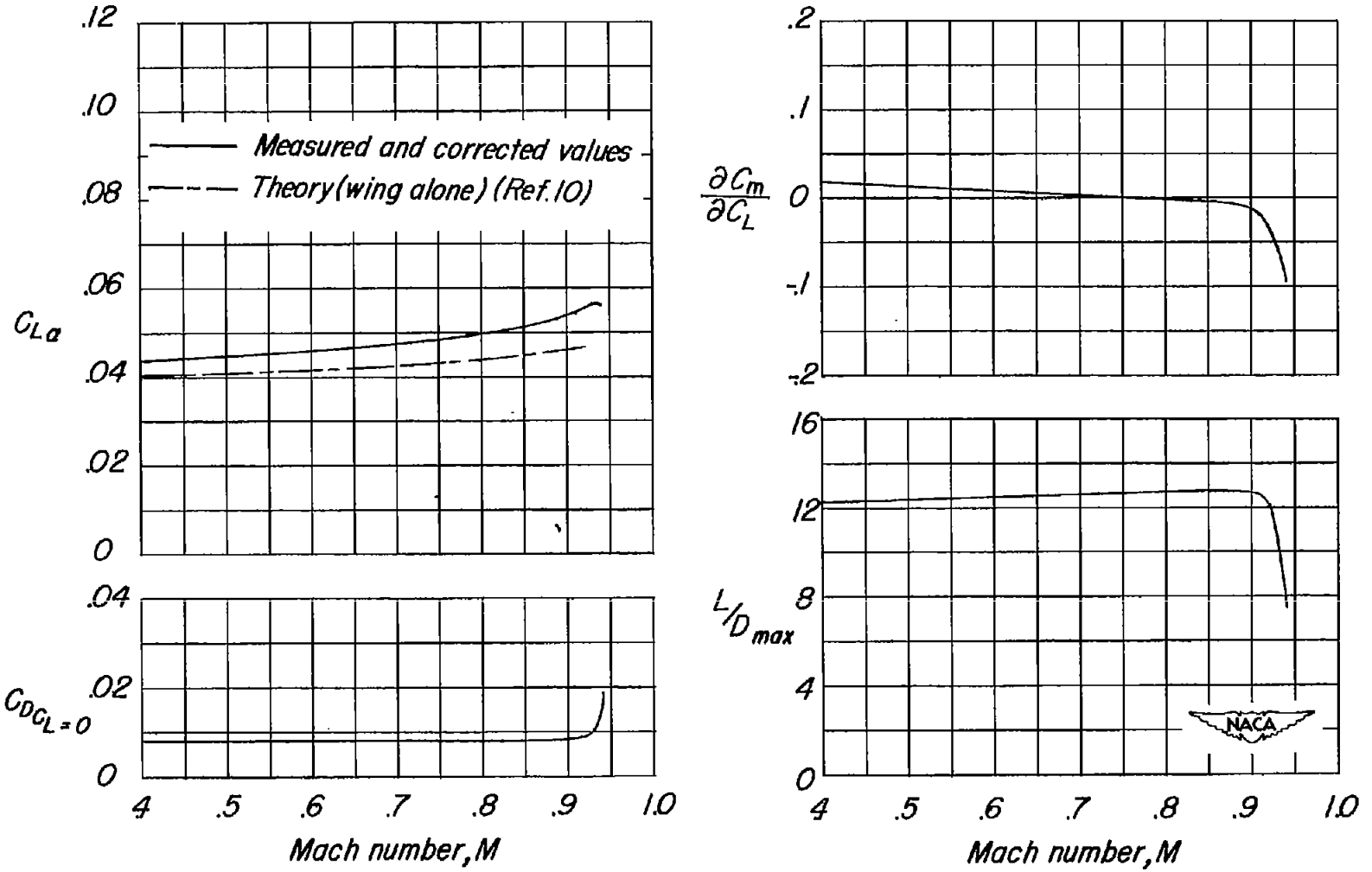

Figure 11.- Summary of the effect of Mach numbers on the aerodynamic characteristics of the 45-2-.6-006 wing-fuselage combination.

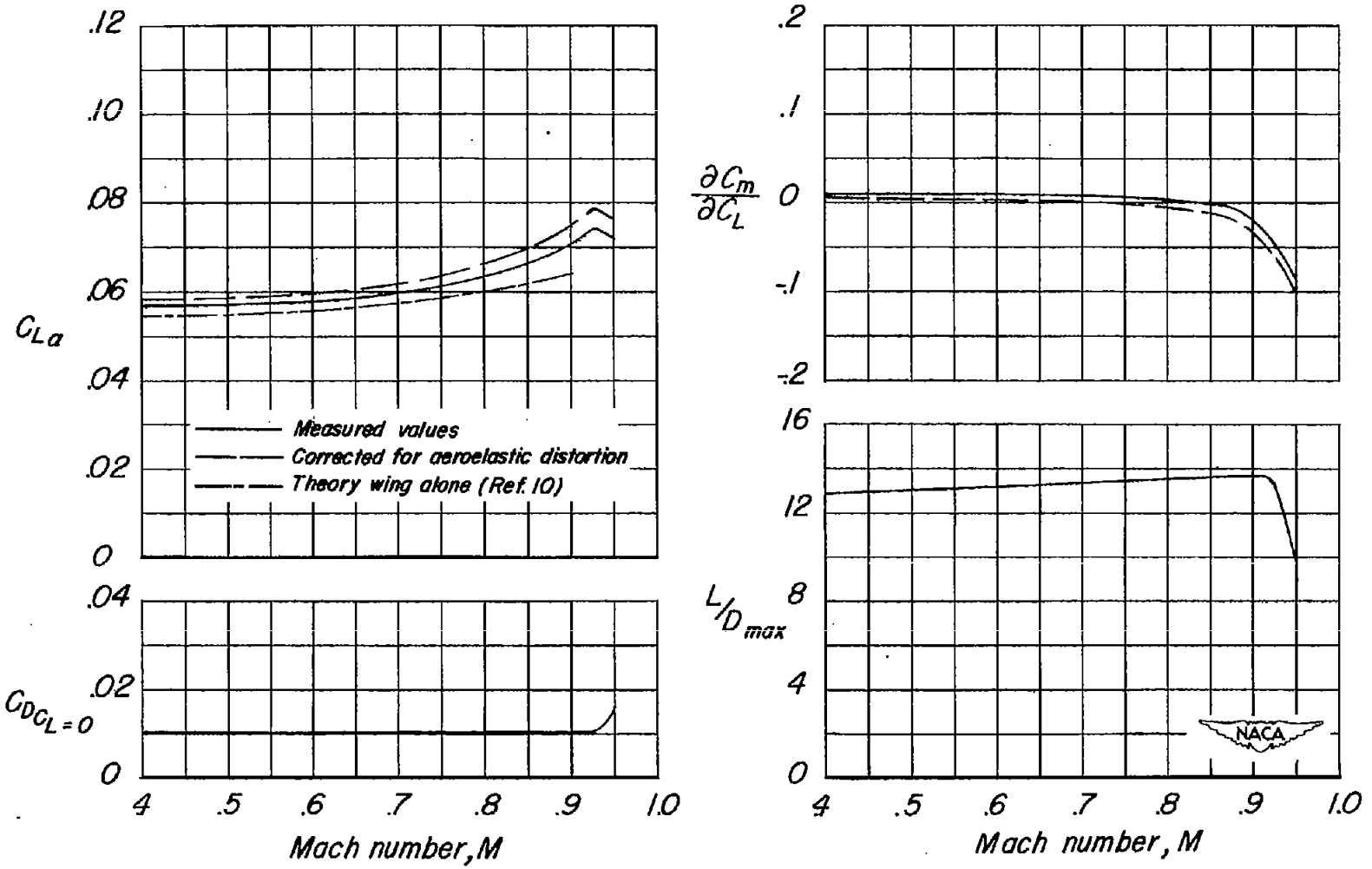

Figure 12.- Summary of the effect of Mach number on the aerodynamic characteristics of the 45-4-.6-006 wing-fuselage combination.

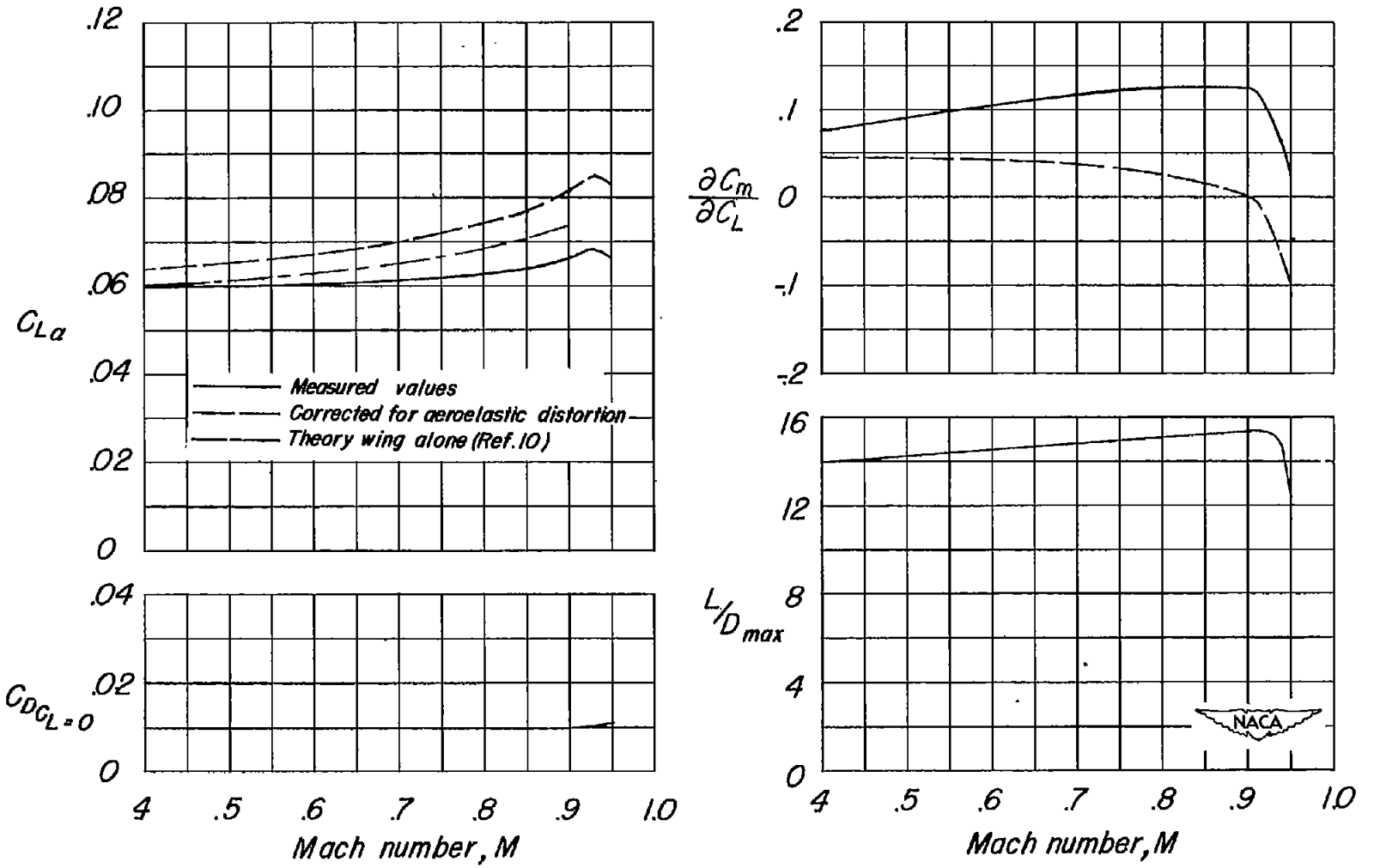

Figure 13.- Summary of the effect of Mach numbers on the aerodynamic characteristics of the 45-6-.6-006 wing-fuselage combination.

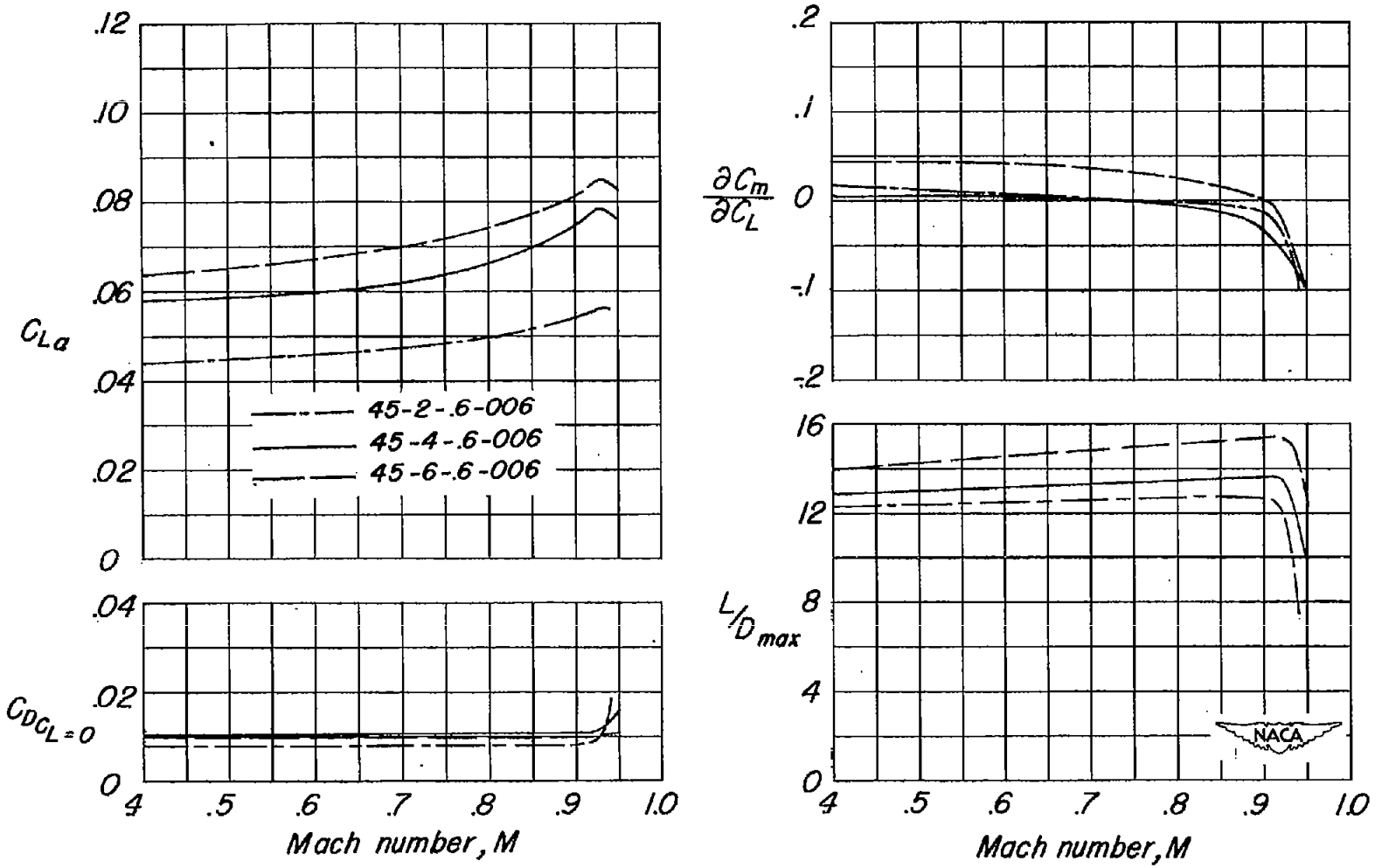

Figure 14.- Comparison of the effects of Mach number on the aerodynamic characteristics of the three wing-fuselage combinations. (C_{L_α} and $\partial C_m/\partial C_L$ corrected for aeroelastic distortion.)

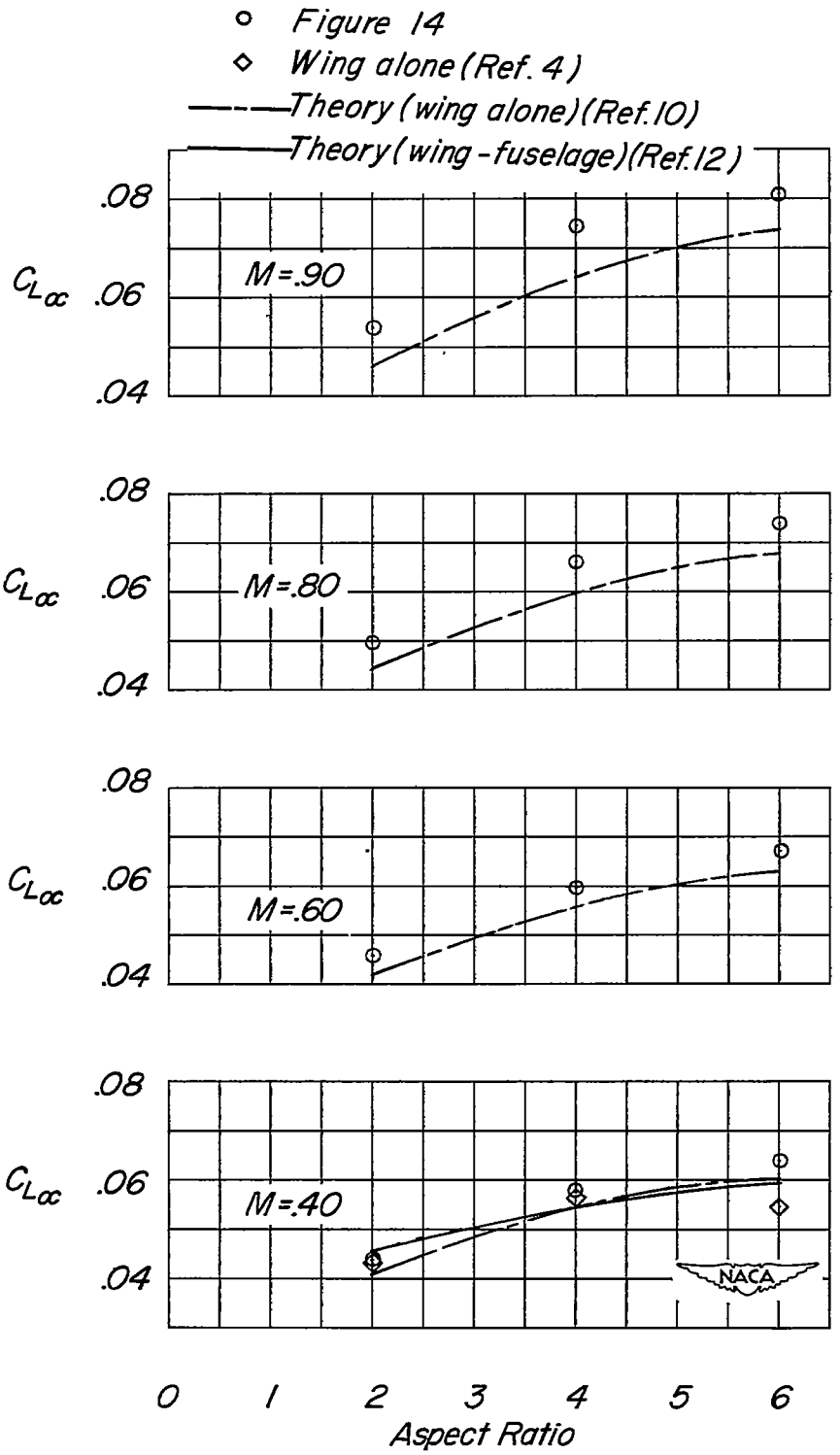

Figure 15.- Effect of aspect ratio on the lift-curve slope at several Mach numbers. (Corrected for aeroelastic distortion.)

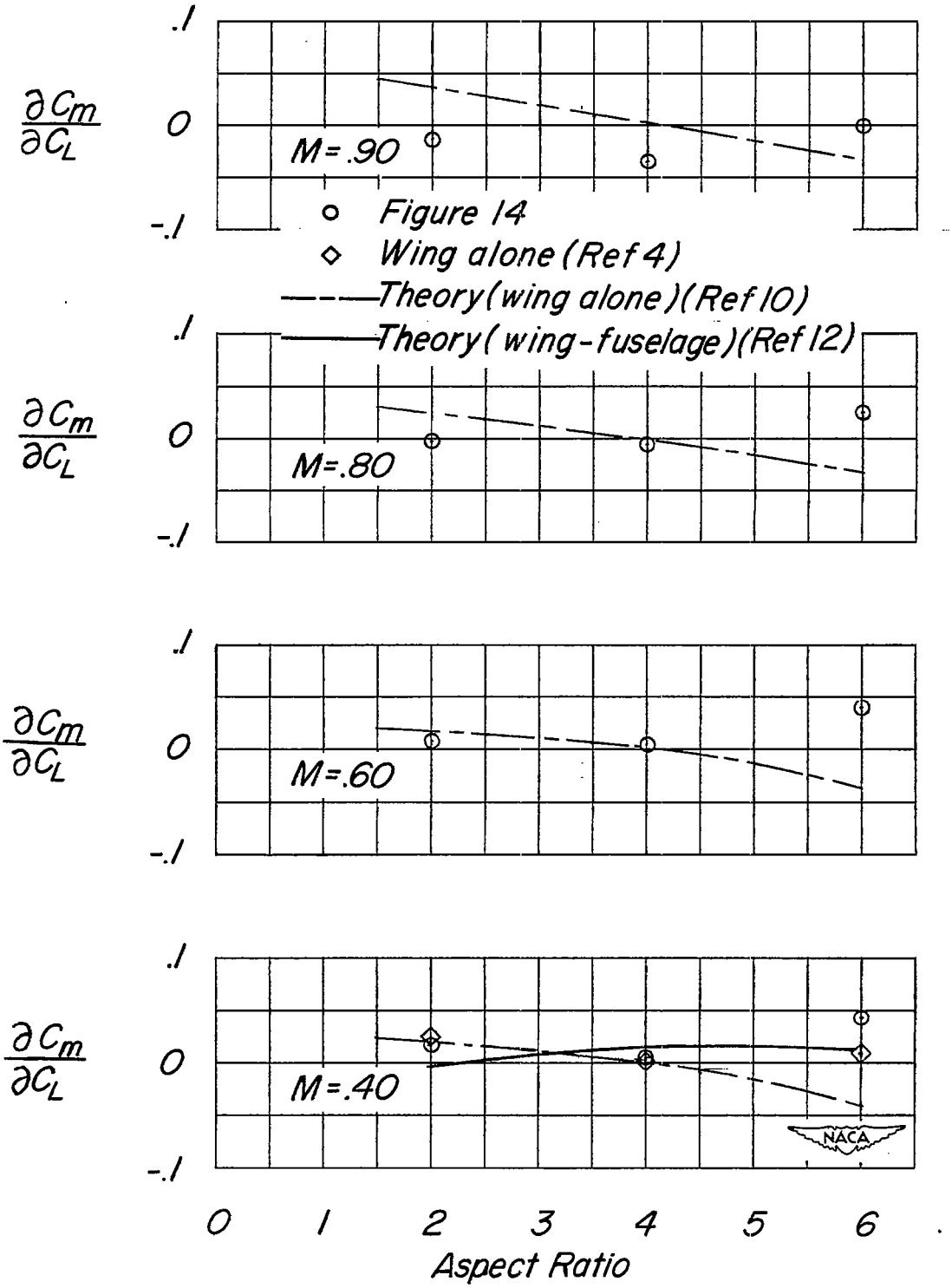

Figure 16.- Effect of aspect ratio on the aerodynamic-center location at several Mach numbers. (Corrected for aeroelastic distortion.)

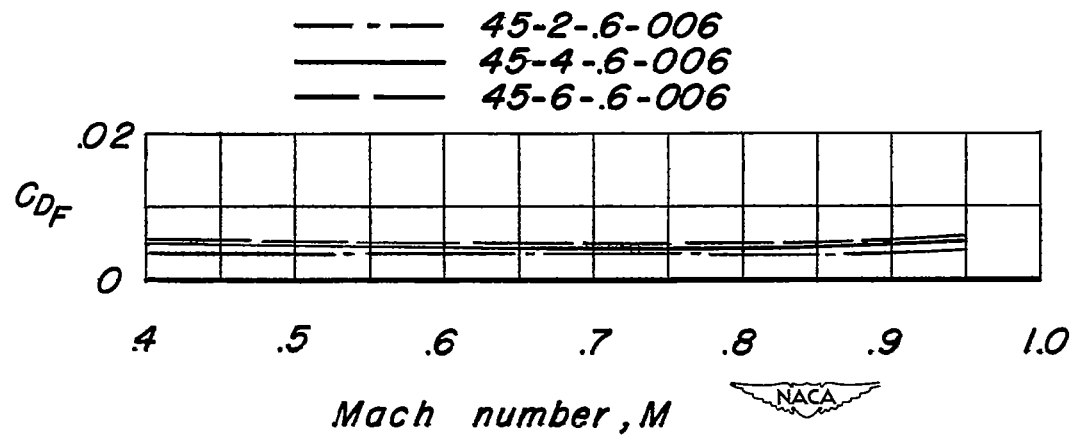

Figure 17.- Comparison of minimum fuselage-alone drag coefficient when based on the respective areas of the three wings.

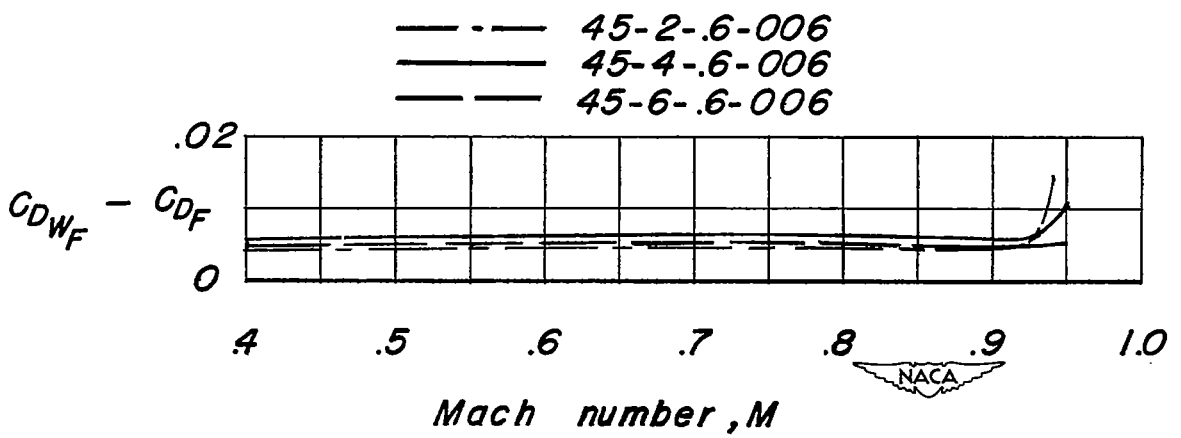

Figure 18.- Variation with Mach number of the wing plus wing-fuselage interference drag at zero lift for the three wings tested.

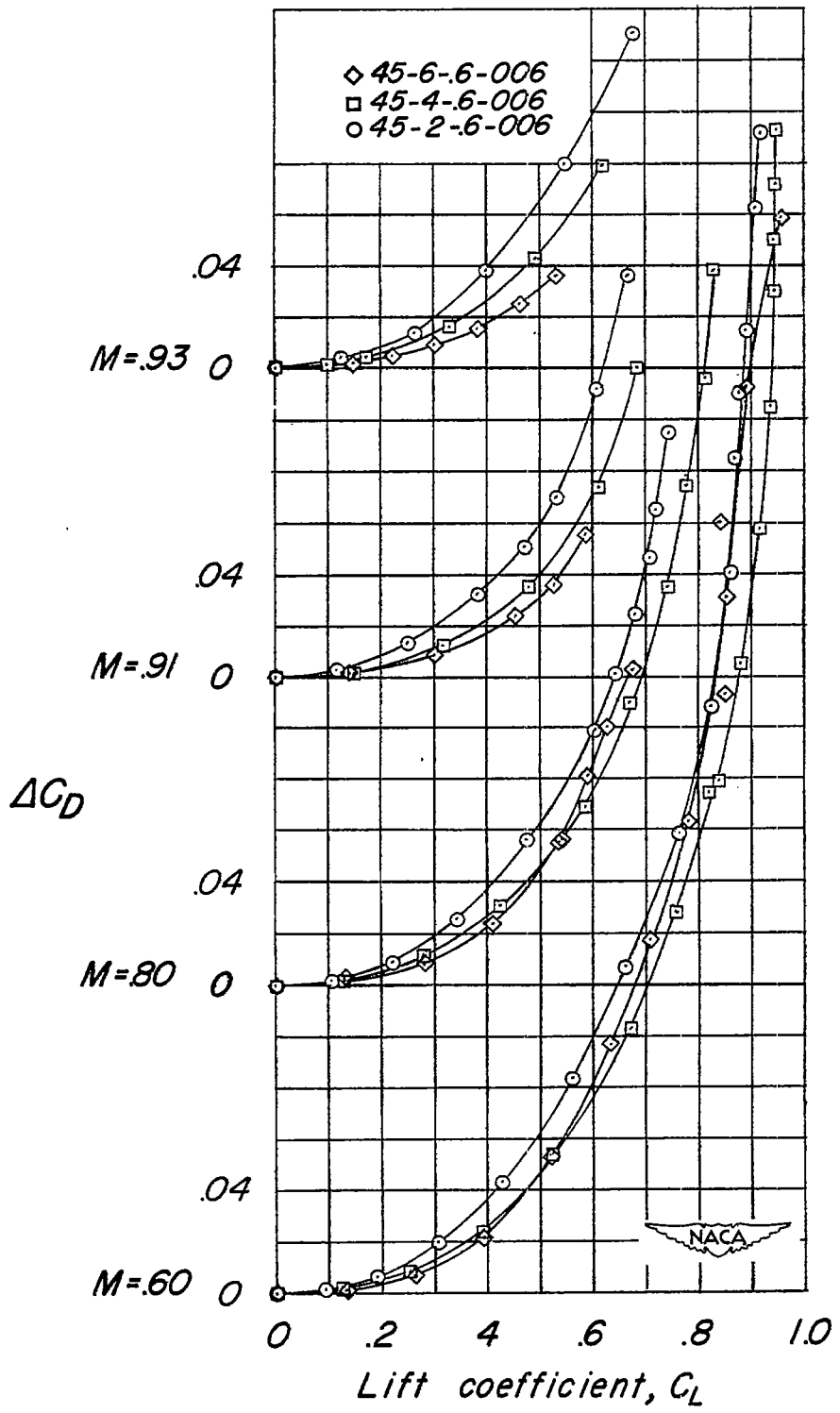

Figure 19.- Comparison of the drag due to lift for the three wings at several Mach numbers.

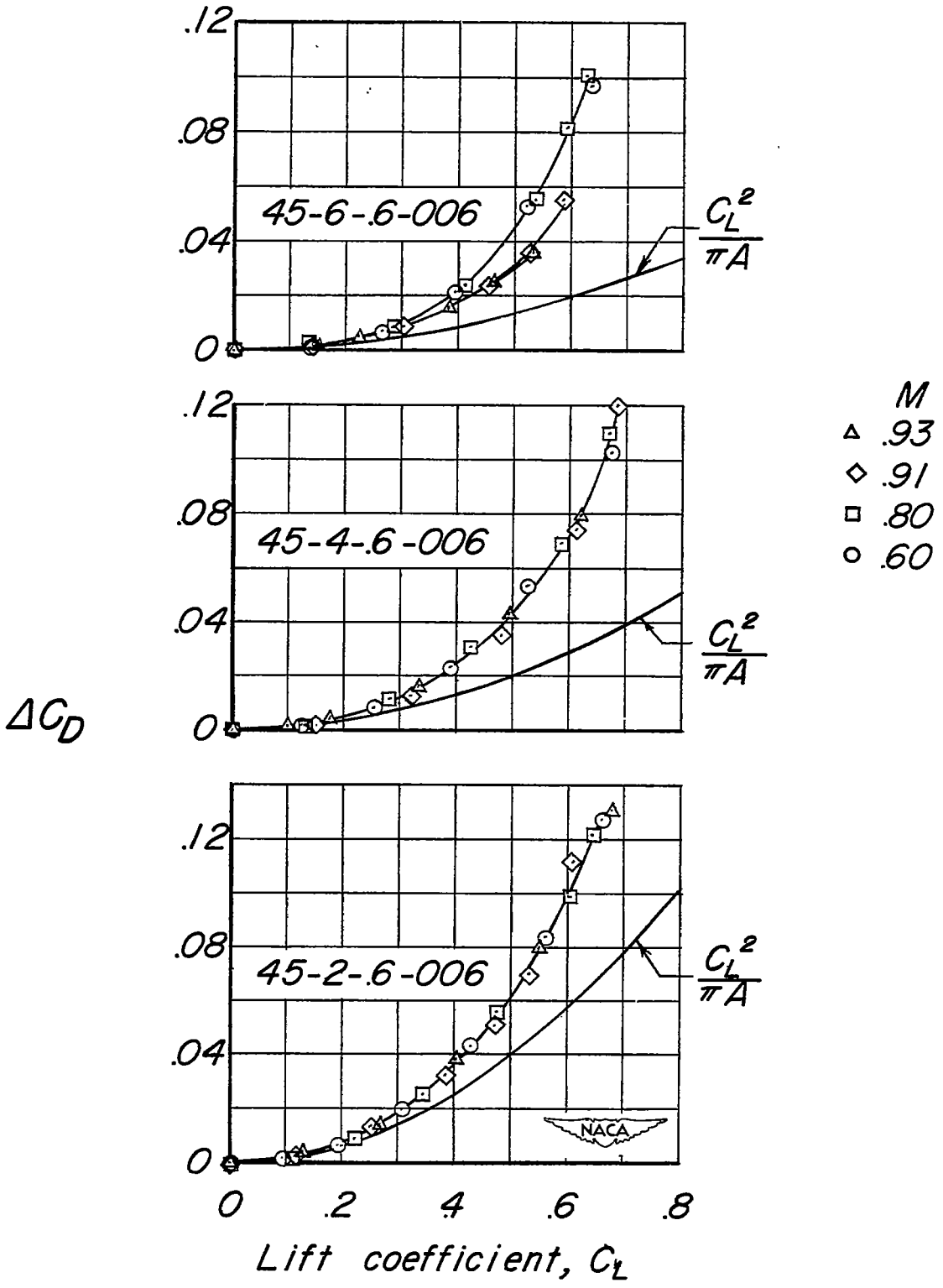

Figure 20.- Effects of Mach number on the drag due to lift.

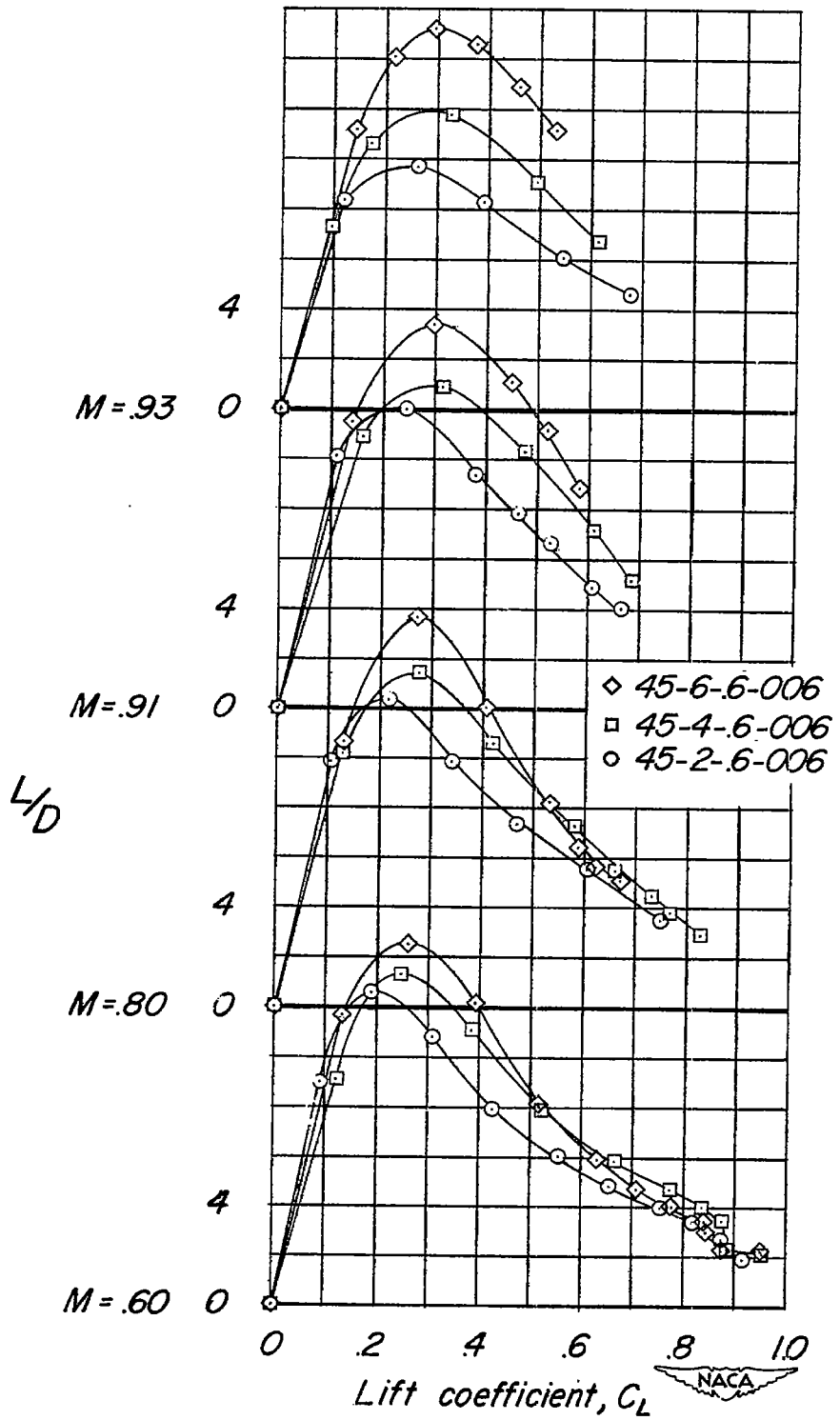

Figure 21.- Comparison of the lift-drag ratios for the three wings at several Mach numbers.